1. Introduction

1.1. Nanotechnology

In recent years, nanotechnology has risen to the forefront of scientific research, thanks to the unique advantages of working on the nanoscale. Nanomaterials are defined as substances smaller than 100nm in at least one dimension (Roco 2003), and the term covers a great many and a large variety of products across many disciplines, although I will be focusing only on their applications within biology.

Nanoparticles have been used as vectors for the transportation of drugs, genes and antigens for immunisation. In addition, they are being used for screening as a diagnostic tool, and are becoming increasingly important in the treatment of cancer. Self-assembly is a feature of some nanoparticles that are of particular importance to this project.

1.1.1. Drug delivery

For many of the problems faced within the field of drug delivery, nanoparticles appear to offer a solution. Their size, pharmacokinetic properties, and potential for surface modification are making them an increasingly appealing prospect within the pharmaceutical industry; consequently research is being conducted on a great number of different nanoparticulate drug delivery systems.

Due to their size, nanoparticles have a very high surface area to volume ratio compared with that of traditional drugs, which yields a greater bioavailability, i.e. a higher proportion of the initially administered drug reaches the blood (Emerich and Thanos 2006), hence providing a more effective treatment. Furthermore, drugs that need to pass through usual problem areas such as the pulmonary system and tight epithelial cell junctions in the skin typically have to be specially designed, but nanoparticles' size means passage through these junctions is not problematic (Emerich and Thanos 2006). When PEGylated (see below), they can also pass through the blood brain barrier (BBB) by binding to the receptor B1 (Kairemo, Erba et al. 2008). Designing drugs able to cross the BBB is traditionally very difficult to do, yet is a prerequisite for their being able to treat diseases such as brain cancer and Alzheimer's disease (Chopra, Gulati et al. 2008).

Perhaps the most important advantage that nanoparticles provide is the scope for surface modification. 'Conventional' nanoparticles, with unmodified surfaces, are quickly cleared from the blood (Grislain, Couvreur et al. 1983) due to an immunogenic process called opsonisation. Blood opsonic factors, for example antibodies or components of the complement system, bind to the surface of the particle, targeting it for clearance by phagocytosis. Traditional drugs also have to be carefully selected and tested to ensure that this does not present a problem for their mode of action. So-called 'second generation' nanoparticles however, are modified to protect against opsonisation, the most common method involves coating the surface in polyethylene glycol (PEG). PEG is a hydrophilic co-polymer which resists opsonisation by sterically hindering opsonins from binding to the surface, thus maximising activity by prolonging the time of the drug in the blood (Boerman, Oyen et al. 1997); this process is known as PEGylation. Another application of nanoparticle surface modification is targeting the drug to a particular cell type, for example epithelial cells, based on the surface profile of the cell (reviewed in (Kim and Dobson 2009)). Consequently, the drug accumulates in the targeted cells, and so is at a high concentration where it is required. This also helps it avoid macrophages (Moghimi, Hunter et al. 2001), prevents drug wastage and reduces side effects, as the drug only affects infected tissues. This is used widely in cancer research (see section 1.1.4. nanoparticles in cancer).

Pharmacokinetics is concerned with how the body affects a drug, and is divided into four areas: absorption, distribution, metabolism and elimination (ADME). Therefore, the most efficient drugs are those which are well absorbed into the blood, distributed to the places where it is needed, and not metabolised or eliminated too quickly (Zolnik and Sadrieh 2009). All the advantages of using nanoparticles in drug delivery that have been discussed so far highlight the optimal ADME properties that nanoparticles have the potential to provide. They also provide a means for possible reformulation of molecules that were previously thought to be good drug candidates, but were not able to be used due to poor pharmacokinetic properties. These could potentially be redeveloped in nanoparticle delivery systems, which would have a very large cost-saving implication for the pharmaceutical industry (Emerich and Thanos 2006).

There are two main types of nanoparticle used for drug delivery: nanospheres and nanocapsules. Nanospheres are matrix systems, in which the drug is uniformly dispersed throughout the particle, whereas nanocapsules are vesicles in which the drug is encapsulated by a polymer membrane (Barratt 2003). Nanoparticles used in drug delivery tend to be made of biodegradable polymers or co-polymers, allowing for slow and sustained release of the drug at the target site over a long period (Singh and Lillard 2009) and subsequently results in no trace of the carrier.

1.1.2. Gene Therapy

Gene therapy involves the transport of a gene into the nucleus of a targeted cell. In nanotechnology this can be done by the use of liposomes which are similar to nanocapsules differing in that their contents are surrounded by a lipid bi-layer instead of a polymer membrane. The advantage of this is that the liposome can pass through the lipid bilayer of the cell, and so remain intact within the cell. Consequently, the gene can be delivered to the nucleus without being damaged by exposure to the cell cytosol (Emerich and Thanos 2006). Several examples of this technology have been published (Liu, Zern et al. 2003) (Zhang, Schlachetzki et al. 2003). The latter of these is an example of targeted gene therapy: the surface of an immunoliposome containing the plasmid was PEGylated and subsequently linked to an antibody for the human insulin receptor (HIRMAb). This targeted the gene to the brain of a monkey, as the antibody allowed it to pass through the BBB via transcytosis and then across the neuronal plasma membrane by endocytosis.

Another possible method of delivering genes is again to use polymeric nanospheres, similar to that used in drug delivery. The gene can be delivered into the cytoplasm, but it has not yet been established how to use this method to transport the gene straight into the nucleus. However, despite this, the method has had some successes (Cohen-Sacks, Najajreh et al. 2002) (Perez, Sanchez et al. 2001).

A third type of nanoparticle used in gene delivery is dendritic or hyperbranched polymers. These conjugate with the DNA by ionic interactions between the negative

phosphate backbone of the DNA and the positive polymer of the nanoparticle (reviewed in (Gillies and Frechet 2005)).

1.1.3. Screening and diagnostics

Molecular screening is used as a diagnostic tool to identify disease, for example in screening for cancer cells. There are two elements of a molecular screening system: recognition and signal transduction. Therefore both of these components must be efficient in order for the system to be successful. Nanoparticles are increasingly being implemented as a novel way to amplify the efficacy of screening systems, making use of the unique optical, electronic and magnetic properties that their cores can provide. They can be used to detect metal ions, proteins, nucleic acids and microorganisms (Agasti, Rana et al. 2010). One of the first types of nanoparticles used in this field was quantum dots (QDs): nanocrystals consisting of a CdSe core with a ZnS shell. QDs are fluorescent nanoparticles, which, once excited, fluoresce in a large range of colours, dependent on particle size. They can be functionalised with antibodies or ligands, which when bound to their substrate, the molecule being screened for, elicit a signal. This has improved the fluorescent markers used for protein detection: traditional markers were short lived, but the signal of QDs decays very slowly and so they last much longer. The markers also used dyes which ran together, leading to difficulty in discriminating between differently stained proteins. QDs however do not have this problem, and consequently several events in a cell can be monitored simultaneously (reviewed in (Medintz, Uyeda et al. 2005)). They can also be used in the detection of other molecules, such as nucleic acids and metal ions (Agasti, Rana et al. 2010).

Another field of nanotechnology used for screening is known as colorimetric detection, which employs nanoparticles that change colour when the ligand is bound or upon clustering. Gold particles are often used for this (AuNPS) and can detect many substrates, such as harmful heavy metal ions (Huang and Chang 2007), proteins (Otsuka, Akiyama et al. 2001) and nucleic acids, where the AuNP is functionalised with a DNA

strand so that a complimentary sequence is recognised and elicits a signal (Thaxton, Georganopoulou et al. 2006).

A final example of the many applications of nanoparticles in this area is a 'bio-barcode' assay. Similarly to colorimetirc detection, an AuNP is linked to DNA. The target oligonucleotide binds, and this is then 'sandwiched' with another AuNP. A magnetic field is used to separate the complex from the target solution, and the DNA is detected (Agasti, Rana et al. 2010). Alternatively a protein or other immunogen can be detected if the AuNP is attached to a monoclonal antibody.

1.1.4. Nanoparticles in cancer

Cancer research is, of course, a highly important field, and so it is no surprise that it is an area in which nanotechnology is being implemented ever more. Similarly to the rest of medical biology, the areas that can most benefit from the use of nanoparticles are drug delivery and imaging (Kairemo, Erba et al. 2008).

Anticancer drugs, usually more so than other drugs, need to be targeted to the tumour site, as they can have adverse effects on normal tissues. Therefore being able to target nanoparticles offers a significant advantage for using them in drug delivery. There are two ways this can happen: passively or actively. Passive targeting is an option because tumour blood vessels have higher permeability than ordinary blood vessels, in order for the tumour to get enough nutrients (Ferrara and Gerber 2001). Consequently, providing that the nanoparticle stays in the blood long enough, it will accumulate at the tumour site. However, this method is not always feasible, and does not work for larger tumours, in which the vascularisation is poor, and so active targeting can be used instead. Cancer cells tend to overexpress some of their surface receptors (Kim and Dobson 2009) and this can be exploited: 'smart' nanoparticles can be made, displaying a receptor/substrate which binds to the complimentary ligand on the cancer cell. For example, folic acid receptors are overexpressed on cancer cells, and so nanoparticles are being developed which display folic acid on their surface (Thomas, Majoros et al. 2005). Antibodies can also be used, but to avoid provoking an immune response, either only a

fragment is used, or a non-binding region is modified with a human region (Kim and Dobson 2009).

The other area in which nanoparticles can be implemented within cancer research is in imaging. Magnetic resonance imaging (MRI) is a useful technique for indentifying tumour tissue. The tumour must be highlighted with a contrast agent in order to be seen, and nanoparticles can be used to do this, for example, a nanoparticle consisting of a PEGylated iron centre, which disturbs the magnetic field by containing a magnetic moment (Kairemo, Erba et al. 2008). Another way in which nanoparticles may be used in imaging is with ultrasound. Traditionally, ultrasound uses only the excitation of minute gas bubbles, but solid nanoparticles have also been used in addition to the bubbles to enhance the image (Liu, Levine et al. 2006).

Although many of these nanoparticle functions are still being researched and not yet in use, hopefully in the future nanoparticles will have a large roll in cancer treatment.

1.1.5. Antigen delivery and immunisation

Vaccination can be carried out using live attenuated virus strains, killed viruses or deactivated toxins. However, all of these methods have disadvantages, such as attenuated viruses reverting back to a dangerous form, or toxins producing a poor immunogenic response, in which case it is often better to use the viral antigen to provoke an immune response. The antigen by itself would have a poor level of immunogenicity, therefore it must be linked to an adjuvant, which promotes a stronger immune response. It must also have a carrier: this can be a nanoparticle. Antigens can be delivered, like drugs, in nanocapsules or nanospheres (Lutsiak, Robinson et al. 2002). However, they can also be delivered in a range of other vectors, such as non-replicating viruses, virosomes and calcium phosphate nanoparticles (reviewed in (Peek, Middaugh et al. 2008))

Antigens can also be delivered as part of the nanoparticle itself, as shown by the Burkhard group. Instead of being a vector, in this case, the nanoparticles' activity is intrinsic to their design. They were first invented in 2006, when a monomer was computationally designed with oligermerisation domains that would lead to efficient self-

A.

DEMLRELQETNAALQDVRELLRQQVRQITFLRALLMGGRLLARLEELERRLEELERRLEELERA

B.

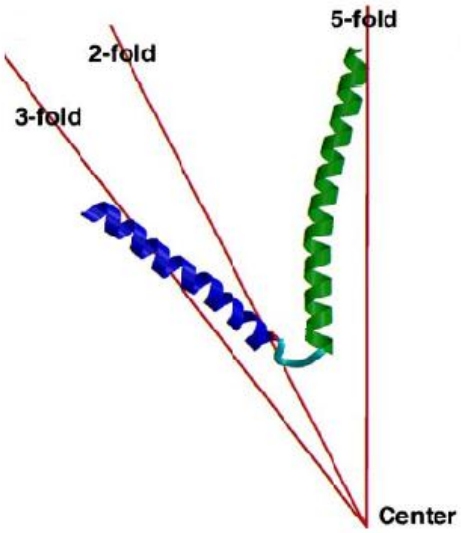

C.

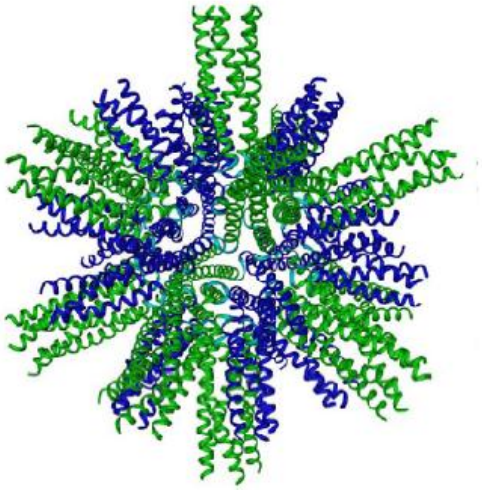

D.

GGGGGGGCAGTGGAGATCCGCCACCTCCCAACCCGAATGACCCACCGCCTCCGAATCCGAACGATTGA
R G G S G D P P P P N P N D P P P P N P N D

Figure 1.1 Composition of the peptide nanoparticles that I will be making.
A. Amino acid sequence of the monomer, excluding his-tag region. Green represents the pentameric coiled-coil COMP domain: blue represents the trimeric coiled-coil domain.
B. The arrangement and symmetry elements of the monomer, with the linker region shown in turquoise.
C. Computer model of assembled 'empty' nanoparticle, composed of 60 monomers.
D. DNA and corresponding amino acid sequence of the peptide in 'empty' nanoparticle, which will be displayed on the surface.
Adapted from (Raman, Machaidze et al. 2006)

assembly (see section 1.1.6. Self-assembly of nanoparticles) into spherical nanoparticles of roughly 16nm in diameter (Raman, Machaidze et al. 2006). The monomer has two domains: a pentameric coiled-coil COMP (Cartilage Oligomerisation Matrix Protein) domain, and a specially designed trimeric coiled-coil domain, joined by a linker region. As shown in Figure 1.1, the monomers self-assemble into a 60-mer with a very high level of symmetry (dodecahedral). The monomer was then engineered to contain a third region, a peptide (Figure 1.1 D) which can be replaced by any other peptide of choice. Once assembled, this region is displayed repetitively on the surface of the nanoparticle. Consequently these nanoparticles were designed as a very efficient antigen presentation system, as not only is the antigen displayed 60 times on one molecule, its high level of symmetry and repetitive antigen display system causes it to resemble a virus and therefore elicit an increased immune response relative to other antigens (Baschong, Hasler et al. 2003). The Burkhard group have so far published two uses for their nanoparticles. The first was to create a vaccine for the SARS virus (which had previously proven difficult), by displaying a region of the B-cell epitope on the surface of the nanoparticle (Pimentel, Yan et al. 2009). The second use was to create actin antibodies, which, due to its highly conserved nature, has again posed a problem in the past. They used a region of actin called the 'hydrophobic loop' which is buried in filamentous actin, but exposed in soluble actin (Schroeder, Graff et al. 2009). For the first time antibodies were made able to detect specifically the levels of soluble actin in the cell. This is called a neo-epitope.

1.1.6. Self-assembly of nanoparticles

Historically in nanotechnology, photolithography (using light to etch onto surfaces) has been used to create two-dimensional nanostructures (Rajagopal and Schneider 2004). This is known as a 'top down' approach. However, an alternative, is molecular self-assembly, defined as the 'spontaneous diffusion and specific association of molecules dictated by non-covalent interactions' (Rajagopal and Schneider 2004). In nature, the self-assembling of identical subunits to produce bigger structures (a 'bottom up' approach) is a process widely observable. Examples include some components of the

cytoskeleton, bacterial extracellular and intracellular protein layers and viral capsids (Papapostolou and Howorka 2009). First proposed by Richard Feynman in 1959, molecular self-assembly based on nature has proven to be an alternative method in synthetic biology for creating three-dimensional bionanostructures (Feynman 1960). Self-assembly offers several advantages. The first is that, as the end product is dictated by the monomers used to create it, it is very easy to adapt or alter the nanoparticle's final structure by simple engineering of the monomer. It also makes the assembly reliable and replicable, as it is governed by molecular interactions and there is no scope for human error. Additionally, the use of enzymes is usually not needed, as all of the assembly information is encoded within the monomer. Consequently, using self-assembly is a very attractive prospect for making nanoparticles, if the material allows.

1.1.7. The nanoparticles used in this project

This project will make use of the nanoparticles created by the Burkhard group (see section 1.1.5. Antigen delivery and immunisation and Figure 1.1). As previously discussed, they were originally designed to be a very efficient antigen display system; however, this will not be their function in this project. They were also designed to self-assemble, which, as explained (see section 1.1.6. Self-assembly of nanoparticles), is very advantageous, as it makes them reproducible, adaptable, and much easer to produce.

1.2. Protein chaperones

Protein chaperones are proteins that mediate the folding, refolding, and prevention of aggregation of other proteins. Unfolded, misfolded or denatured (non-native) proteins have exposed hydrophobic regions which, if left exposed, interact with other non-native proteins, leading to protein aggregation. This is usually irreversible and damaging to the cell. Protein chaperones have their own hydrophobic domains, which they use to bind to these vulnerable exposed proteins and so prevent aggregation from occurring. Most

protein chaperones are expressed constitutively, but for some their expression increases in times of physical stress, for example increased temperature. These proteins are called heat shock proteins (HSPs), whereas constitutive proteins are known as HSCs.

There are four classes of protein chaperones native to humans, each with distinct mechanisms of chaperoning and with varying functions. The chaperonins chaperone the folding of newly translated proteins, as well as the refolding of misfolded proteins. They do this by enclosing the non-native protein within one of two chambers, where the hydrolysis of ATP leads to proper folding. The HSP70s, however, largely chaperone by protecting and folding peptides during translation. They function, with the aid of a co-chaperone, by binding to a hydrophobic site on the peptides. Again, ATP is required for folding. Similarly, the HSP90s require both co-chaperones (sometimes HSP70 itself) and ATP to function, but they play a more regulatory role within the cell, and thus chaperoning occurs slowly. They, again, bind to the chain of peptide, but unlike HSP70, they have a 'lid' region which closes to allow chaperoning. The last class of chaperone is the sHSPs, which do not actively fold non-native proteins, but instead protect them by binding to them, before passing them to one of the other chaperones; this is an ATP-independent process.

Therefore, it is easy to see that all of the different chaperones work together in a cell, and all are required to ensure the proper folding of all proteins (Hartl and Hayer-Hartl 2002).

1.2.1. Chaperonins

The chaperonins are an essential group of protein chaperones, seen in all three organism kingdoms, and present in both cytosol and organelles. They are known to interact with 10% of newly synthesised cellular proteins (Spiess, Meyer et al. 2004). Chaperonins carry out the final step in the journey from DNA to native protein, following transcription and translation, by facilitating the ATP-dependent folding of the completed nascent peptide, if not already folded (Horwich, Fenton et al. 2007). They also function to refold misfolded proteins. In humans there are two classes of chaperonin, divided evolutionarily. Type I,

which has its origins in bacterial cytoplasm, is present in organelles such as mitochondria (HSP60). Type II, originating from archaebacterial cytoplasm, is present in eukaryotic cytoplasm (CTT/TRic). The two types are structurally different, so although they have similar activity mechanisms, their encapsulation mechanisms are different (Horwich, Fenton et al. 2007).

Chaperonins are large (about 800 kDa), complex structures, consisting of two rings. Each ring encloses a cavity, which are the active sites. When the cavity is open, it is overwhelmingly hydrophobic, and so binds unfolded or misfolded proteins, as these also have exposed hydrophobic regions. Once a substrate is bound, ATP also binds, causing a conformational change of the chaperonin. The cavity expands, is sealed, and becomes largely hydrophilic, promoting the proper folding of the protein. Subsequently, the ATP is hydrolysed to ADP, a new substrate and ATP bind to the opposite cavity, and the ADP and folded protein are released (Lucent, England et al. 2009). If the protein is still not folded correctly, it goes through the cycle again. Even if the protein has to go through this process several times, it is still more efficient for the cell than making a new protein (Spiess, Meyer et al. 2004).

Exactly how the protein is folded within the enclosed cavity is unknown, although several mechanisms have been discussed (reviewed in (Lucent, England et al. 2009)). The Anfinsen cage model postulates that the chaperonin does nothing actively to help folding, preventing protein aggregation by merely isolating it until it is properly folded (Ellis 1994). A second model, the iterative annealing model, suggests that the cavity acts as an unfoldase, aiding the folding of a kinetically trapped protein by giving it several attempts at folding properly (Weissman, Kashi et al. 1994). A third model proposes that instead the cavity surface acts as a foldase, providing an environment which promotes quicker folding than would be possible were the protein free in the cytosol (Brinker, Pfeifer et al. 2001). There is evidence to support all of these models, and in actuality, the mechanism could be a mixture of the three, depending on the substrate. However, as mentioned previously, this constitutes just one of several chaperone mechanisms within the cell.

1.2.2. The HSP70 system

The HSP70 family of protein chaperones in humans consists of 13 HSP70s and four related HSP110s. HSP70s have two regions: the N-terminal nucleotide binding domain (NBD), which has ATPase-activity, and the C-terminal substrate binding domain (SBD) (Saibil 2008). They carry out many functions in the cell, often, but not always, in conjunction with a co-chaperone, and can be found in the ER (BiP) and mitochondria (mtHSP70) as well as the cytosol (Hsc70) (Meimaridou, Gooljar et al. 2009).

Like chaperonins, HSP70s function to mediate the ATP-dependent folding of post-translational nascent peptides, although unlike chaperonins, they can also fold co-translationally. Their method of chaperoning, however, is very different; the basic process is as follows. Once bound to ATP, the SBD of the HSP70 binds to a target region of a client peptide, for instance, a nascent peptide that has just been translated. The target region consists of roughly five to seven hydrophobic residues flanked by hydrophilic ones; a pattern which occurs statistically about every 40 amino acids. HSP40 acts as a co-chaperone which presents client peptides to HSP70. Once bound, ATP is hydrolysed to ADP, a process regulated by HSP40, causing HSP70 to clamp onto the peptide in a conformational change. Consequently, the hydrophobic region is no longer exposed, and proper folding can occur without the risk of aggregation. The complex in this form is stabilised by Hip, another co-chaperone. The next step is for Bag, a nucleotide exchange factor, to release ADP, along with the folded protein and complete the cycle. If the protein has not been correctly folded, it can undergo multiple cycles until the folding has been completed (Meimaridou, Gooljar et al. 2009) (Hartl and Hayer-Hartl 2002) (Witt 2010). Again, the exact details of the mechanism of protein folding are unknown.

Aside from this housekeeping protein folding function, the HSP70s also have many other roles within the cell. Co-chaperone domains can be seen in modular adaptor proteins, which can be found at membranes and at the cytoskeleton. This localises the chaperone activity of HSP70, allowing it to carry out specific cellular functions such as protein transport, vesicle secretion and recycling and the regulation of large protein complexes in their assembly/disassembly (Young, Barral et al. 2003).

1.2.3. The HSP90 system

Less is known about HSP90 than about the other protein chaperones. Again, it helps with protein folding and prevents aggregation, but the substrates of HSP90 are less varied than for the other chaperones. HSP90 molecules consist of three regions: the N-domain, which contains the ATP binding site and a 'lid', a linker region and M domain and the C-terminal dimerisation domain (Wandinger, Richter et al. 2008). Like HSP70, HSP90 is assisted by a number of co-factors and co-chaperones, and in fact, for some of its substrates, is assisted by HSP70 itself. In these cases, HSP70 stabilises the substrate in a conformation which then allows HSP90 to bind to it (Scheufler, Brinker et al. 2000).

The details of the process of protein folding are only partially known, but the cycle can be outlined. Once the substrate has passed from HSP70 to HSP90, ATP binds to the N-terminal of each monomer and causes the dimer to close and the lids to shut. The N-terminals dimerise, forming a stable complex. The ATP is then hydrolysed by the co-factor Sba1, allowing the monomers to reopen. The ADP and substrate are released. As for the other chaperone cycles, if the substrate is not folded after one cycle it may undergo more (Wandinger, Richter et al. 2008).

HSP90 also plays a regulatory role by inducing conformational change and hence activating and stabilising proteins (Jakob, Meyer et al. 1995), and so in turn its activity must be regulated. This regulation occurs in three ways (reviewed in (Wandinger, Richter et al. 2008). Firstly, the hydrolysis of ATP to ADP is very slow, in humans this occurs only once every 20 minutes (McLaughlin, Smith et al. 2002). This is because the conformational change resulting in the closure of the complex takes time; however, this delay implies a rate limiting step. Additionally, HSP90 is tightly regulated by all the co-factors that it requires. Lastly, regulation occurs by way of post-translational modifications, such as phosphorylation: increased temperature leads to higher HSP90 phosphorylation, which in turn increases activity (Leesmiller and Anderson 1989).

1.2.4. The sHSPs

The small heat shock proteins (sHSPs) are a family of protein chaperones, whose subunits vary in size between 12 and 40 kDa. Unlike all the other protein chaperones, they do not require ATP for their activity: they protect non-native proteins from aggregation but do not actively fold them. Their function is especially critical in times of physiological stress, when they play an important role in preventing irreversible aggregation until conditions revert to normal and the protein is passed to an ATP-dependent chaperone for folding. While the structures of the sHSPs vary, they all contain a 100 amino acid conserved sequence, the α-crystallin domain (ACD). It is possession of this domain that defines them as sHSPs: it is essential for dimerisation, oligomerisation and chaperone ability. The ACD is always flanked by a variable hydrophobic N-terminal domain, responsible for substrate binding and a C-terminal tail containing a conserved sequence, which largely lacks secondary structure and hyrodrophobicity. The protein chains of the sHSPs dimerise, and self-assemble to form oligomers: it is thought that there is equilibrium between the dimer and the oligomer. Depending on the specific sHSP involved, the oligomers can be homomeric or heteromeric, regular or polydisperse and can range in size between 9 and 50 subunits (Mchaourab, Godar et al. 2009) (Sun and MacRae 2005) (Haslbeck 2002) (Nakamoto and Vigh 2007). Although these oligomers are formed, kinetic studies have shown that they are dynamic and undergo subunit exchange (Bova, Ding et al. 1997). The sHSPs have proved very difficult to crystallise, and consequently little is known about their structure or mechanism of chaperoning. Two aspects of sHSPs will be discussed in more detail: structure, using HSP16.5, from the hyperthermophilic archaebacterium, *Methanococcus jannaschi*, and HSP16.9 from wheat, as they are the only two which have been crystallised: and chaperoning, largely using αB-crystallin, as it is the archetypal sHSP and has been the subject of the most research.

1.2.4.1. Structure – HSP16.5 and HSP16.9

The structure of HSP16.5 could be determined using crystallography. The structure is a sphere consisting of 24 subunits, all paired into dimers (Kim, Kim et al. 1998). It has three sets of eight subunits (Figure 1.2A) and octahedral symmetry. The sphere is hollow, like the chaperonins, but without an entrance. The surface has 14 'windows', eight trigonal and six square, which are large enough to contain small enzymes and polypeptides. The surface is 22% hydrophobic, although the locations of the N-terminal extensions could not be determined from the crystal structure.

The structure of HSP16.9, which also forms monodisperse oligomers, is quite different (van Montfort, Basha et al. 2001). It is a eukaryotic sHSP, as opposed to the prokaryotic HSP16.5. It has 12 subunits, again made of dimers, but instead of a sphere

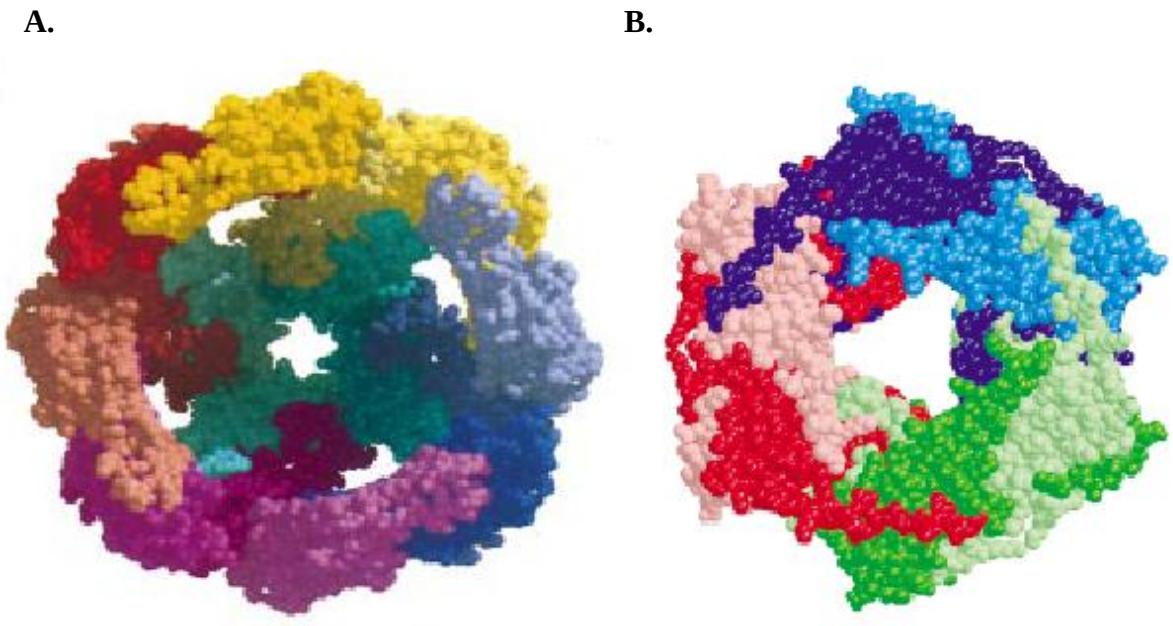

Figure 1.2 Space fillings models of HSP16.5 and HSP16.9.
A. Space filling model of the structure of HSP16.5, an oligomer of 24 subunits. The front 1/3 is removed to show the hollow interior. It is colour coded in tetramers, with each subunit in the tetramer represented by a different shade of the same colour. Taken from (Kim, Kim et al. 1998)
B. Space filling model of the structure of HSP16.9, an oligomer of 12 subunits. It shows one of the two disks; again, different subunits of the same dimer are represented by a different shade of the same colour. Taken from (van Montfort, Basha et al. 2001).

they form a double disk structure, with each disk encompassing six subunits. The structure is shown in Figure 1.2B.

The small size and spherical nature of the sHSPs indicate a marked similarity between these protein chaperones and nanoparticles. Therefore, although they are not synthetic, the sHSPs could also be considered as nanoparticles.

There is no crystal structure available for αB-crystallin because the polydisperse nature of its assembled state means there is no regular unit, however fragments have been crystallised. Recently, solid-sate NMR has been used for αB-crystallin characterisation, and has given insight into the structure of the dimer, showing a new curved shape, (Jehle, Rajagopal et al. 2010) leading to predictions of the oligomeric structure. However, this still only uses average subunit numbers due to polydispersity. Data like this, along with rough structures predicted from homology with the two known sHSP structures is the closest to the actual structure that has yet been achieved.

1.2.4.2. The chaperone mechanism - αB-crystallin

The size of the αB-crystallin subunit is about 20 kDa. It exists predominantly in the lens of the eye, where it forms a heteromer with its homolog, αA-crystallin. Together they make the sHSP α-crystallin, a polydisperse oligomer, whose size ranges from about 200 kDa to 800 kDa. α-crystallin makes up about 50% of the lens proteins, and helps to maintain lens transparency by preventing aggregates from forming. While αA-crystallin is found only in trace amounts in non-lens tissues, αB-crystallin distribution is ubiquitous (Augusteyn 2004).

As mentioned above, the exact mechanism by which αB-crystallin carries out its chaperone function is still unknown. The first step in determining the mechanism is discovering the binding sites for both substrates and oligomerisation. Ghosh and Clark used protein pin array technology to identify the oligomerisation sites on the αB-crystallin monomer (the binding sites to αA-crystallin and αB-crystallin) (Ghosh and Clark 2005). The sites were present in all three of the domains, and were similar to sites known to be important for substrate binding: as is the nature of protein chaperones, proposed binding

sites are hydrophobic. The N-terminal, especially, is thought to be important for both oligomerisation and substrate binding (Aquilina and Watt 2007), since the removal of the N-terminal of the yeast sHSP, HSP26, resulted in loss of both oligomerisation and chaperoning; although clearly one could be the result of the other (Haslbeck, Ignatiou et al. 2004).

Like the other protein chaperones, it is thought that sHSPs bind to a large range of substrates. However, there are several sHSPs (in humans there are ten) and different sHSPs are found in the same cellular locations, suggesting that they have different specificities for different clients. This idea is backed up by the fact that the N-terminal is the most variable region of the sHSPs, and it is this region that largely governs substrate binding (Haslbeck, Franzmann et al. 2005), although there is some variation in the C-terminal tail which is also thought to contribute to client selection (Ghosh, Shenoy et al. 2006).

It is not yet known whether substrate binding involves a conformational change, subunit exchange or dissociation of the oligomer; at least one of these mechanisms must be implicated if the same sites are used for oligomerisation and substrate binding. Additionally, the crystal structure of wheat HSP16.9 shows that the hydrophobic regions of the N-terminal are buried in the oligomer (van Montfort, Basha et al. 2001), and so clearly they must be liberated in order to bind to non-native proteins. However, this does not necessarily hold true for all sHSPs.

sHSPs are dynamic oligomers, and thus exchange subunits constantly, as can be demonstrated in several ways. For example, mass spectrometry has been used to monitor oligomer size of α-crystallin, where it was found to change following the loss or gain of a subunit (Aquilina, Benesch et al. 2005). Thus, it could be that the subunits bind substrate during this process, when they are dissociated and all of the binding sites are exposed (Lindner, Kapur et al. 1998). This is supported by observations that under stressful conditions, which trigger higher chaperone activity in sHSPs, there is an increase in hydrophobicity. Further evidence for this theory can be found in Surface Plasmon Resonance (SPR) data from Liu et al (Liu, Ghosh et al. 2006), which shows that increased subunit dynamics, caused by thermal stress, leads to increased chaperoning: a result already previously shown for αA-crystallin (Bova, Ding et al. 1997). However, there is

data that contradicts this model: the subunits of HSP26 were crosslinked together to prevent subunit dissociation, but chaperoning was still observed (Franzmann, Wuhr et al. 2005). Similarly, Aquilina et al. showed that when αA-crystallin is mutated to decrease subunit dynamics, the rate of chaperoning is not affected (Aquilina, Benesch et al. 2005). These results suggest that it is not subunit dissociation but another mechanism, perhaps a change in conformation, which allows substrates to bind to the binding sites. Whether the chaperone mechanism is universal for all sHSPs is unknown.

sHSPs bound to their substrates do not exist freely, but are instead still in stable complexes. The substrates are held in these complexes and so cannot aggregate. One sHSP can bind up to one substrate per subunit, which is much more efficient than the other protein chaperones (Haslbeck, Franzmann et al. 2005). In the lens it has been proposed that this is irreversible (Horwitz 2003), and once substrates are bound in these

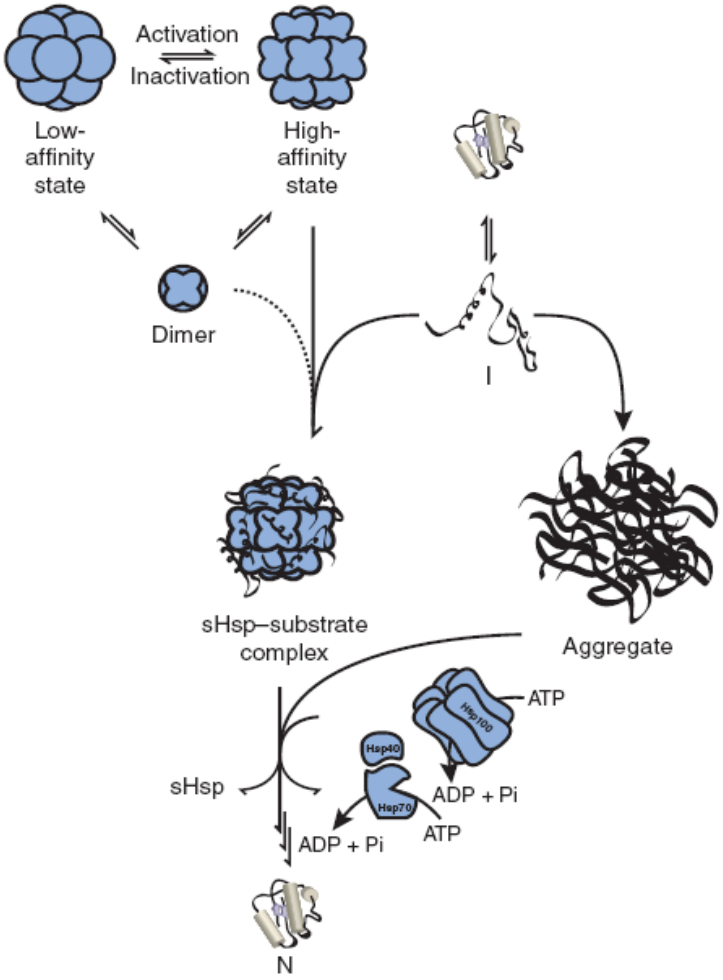

Figure 1.3 Proposed model of the mechanism of sHSP chaperoning.
The sHSP oligomer either changes conformation or a subunit dissociates in order to bind to the non-native protein. The sHSPs bound to their substrates form a complex to prevent aggregation until an ATP-dependent protein chaperone refolds the protein and liberates the sHSP. Taken from (Haslbeck, Franzmann et al. 2005)

complexes, they remain there. This is because the lens is a closed, avascular system, lacking organelles and with a very specific protein profile. The α-crystallin simply prevents the non-native proteins from compromising the optical properties of the eye, but it cannot refold them. In other cells, however, this would not make sense, as they possess the ability to refold the proteins. Therefore they are transferred instead to other protein chaperones, and with the help of ATP, refolded (Lee and Vierling 2000). A general outline of the mechanism of sHSPs is shown in Figure 1.3.

1.2.5. Nanoparticle chaperones

The implementation of nanoparticles as synthetic chaperones is a subject that has received interest in the last decade. As previously mentioned, the surface of nanoparticles can usually be easily modified, and can thus be adapted to have chaperoning properties. The small size of nanoparticles means they also have a very high surface area to volume ratio, and thus any surface property which they possess will be displayed at a relatively high level. Therefore if nanoparticles can be developed to have chaperone properties, they will potentially be very efficient chaperones. However, it is not simply a case of the smaller the better, as if the nanoparticle is too small the curvature will be too big for the substrate to bind well to it, and so a compromise is reached at nanoparticles at the larger end of the scale (Fei and Perrett 2009).

Biological chaperones bind to their substrates through hydrophobic interactions between their own hydrophobic regions and those of their clients. This concept has been used in nanotechnology, using amphiphilic polymers modified with hydrophobic groups that self-assemble into micelle-like particles (Cavalieri, Chiessi et al. 2007). Usually the polymers would form micelles with a hydrophobic core and hydrophilic surface, but the addition of the hydrophobic groups causes them to be displayed. Consequently the surface of the nanoparticle is hydrophobic, allowing it to chaperone non-native proteins. Nanoparticles have also been made that interact with non-native proteins in a different way: by displaying charged functional groups on the surface, a nanoparticle can bind to the substrate using electrostatic interactions instead of hydrophobic ones. One example of

this is a gold nanoparticle, functionalised with 2-(10-mercaptodecyl) malonic acid (AuDa), which is very negatively charged (De and Rotello 2008). It was tested on three proteins, all of which were denatured thermally, and the nanoparticles not only prevented their aggregation, but assisted with their refolding. They were dissociated using NaCl, and the substrates' enzymatic activity was restored. Raghava et al provided another example of this, using simple, unmodified titanium oxide ($Ti0_2$) nanoparticles (Raghava, Singh et al. 2009). These provided similar results to the gold nanoparticles: they prevented aggregation, assisted refolding, and upon the addition of NaCl, dissociated, resulting in the original functional substrate.

The examples of nanoparticle chaperones discussed so far all have a similar mode of action to that of sHSPs. Utilising a different approach, nanoparticles in the form of a nanogel have been developed to function more like the chaperonins (Akiyoshi, Sasaki et al. 1999) (Nomura, Ikeda et al. 2003). Pullulan bearing a cholesterol group (CHP) self-aggregates in water to form the nanogel, which traps non-native proteins (denatured thermally or chemically using GdmCl) within. Once refolded, β-cyclodextrin triggers the release of the substrate, and so is acting in a similar manner to a co-chaperone or ATP.

Therefore, overall, nanoparticles can have the capability to act as good protein chaperones, an area which requires further investigation.

1.3. This project

1.3.1. The Burkhard nanoparticles as chaperones

Section 1.2.5 demonstrates that nanoparticles can act as very effective protein chaperones, as do the non-synthetic sHSPs. The purpose of this project, therefore, is to investigate whether the peptide nanoparticles developed by the Burkhard group also work as good protein chaperones.

The nanoparticles that will be utilised are composed almost entirely of coiled-coils (Figure 1.1). Coiled-coils are stabilised by a 'knobs into holes' interaction model, first

proposed by Crick (Crick 1953) in which apolar side chains pack into a hydrophobic core (Burkhard, Stetefeld et al. 2001). The *de novo* trimeric coiled-coils designed by the Burkhard group are especially stabilised by hydrophobic interactions between coils, and contain a hydrophobic seam running along the length of them (Raman, Machaidze et al. 2006) (Burkhard, Meier et al. 2000). The pentameric coiled-coils from the COMP protein again use hydrophobic interactions, and it actually contains a long hydrophobic indent (Malashkevich, Kammerer et al. 1996). As protein chaperones use hydrophobic regions to bind to hydrophobic regions on their substrates, this means that, although designed with a different purpose in mind, these nanoparticles could function as efficient protein chaperones.

Furthermore, these nanoparticles display a small peptide on their surface (Figure 1.1D). This peptide contains a large number of prolines, which will cause it to lack secondary structure. Its amino acid sequence also renders it neutral and lacking hydrophobicity. This peptide can thus be compared to the C-terminal tail of αB-crystallin, which shares similar features, and so this peptide could perhaps also provide chaperone activity.

It is easy to see similarities between the spherical structure of the sHSPs, especially the crystallised structure of HSP16.5, and that of these nanoparticles. Consequently, a sHSP would serve as a good control for the nanoparticle.

1.3.2. Nanoparticles enhanced with αB-crystallin sequences

Additionally the nanoparticles will be enhanced with regions of αB-crystallin, which are solvent exposed and known to be substrate binding sites to find out if this improves their chaperone ability.

As described earlier (section 1.1.5. Antigen delivery and immunisation), these peptide nanoparticles can be modified. The monomer peptides can be adapted to replace the existing displayed peptide with any other peptide sequence, which will then, in theory, be displayed on the surface of the nanoparticle 60 times once it has self-assembled. Therefore, if sequences of αB-crystallin that are thought to be important to its chaperoning

(i.e. the substrate binding sites), are the sequences used then these regions will be displayed on the surface of the nanoparticles (see Figure 1.4). This would then potentially create very efficient 'super-chaperones'. Four regions of αB-crystallin were selected for this function, varying in size and sequence. Two (np1 and np3) are shorter peptides, covering one cluster of substrate binding sites, while the other two (np2 and np4) are longer and cover two clusters.

1.3.3. Project outline

Following from the previous two sections, in this project, first the 'empty' nanoparticles (those that do not contain regions of αB-crystallin) will be made and assembled, and then tested for their chaperone function. Subsequently, the DNA of the nanoparticles will be modified to encode regions of αB-crystallin. Four different αB-crystallin-containing nanoparticles will also be made, assembled and tested for chaperone function.

Transmission Electron Microscopy (TEM) will be used be check the assembly of the nanoparticles.

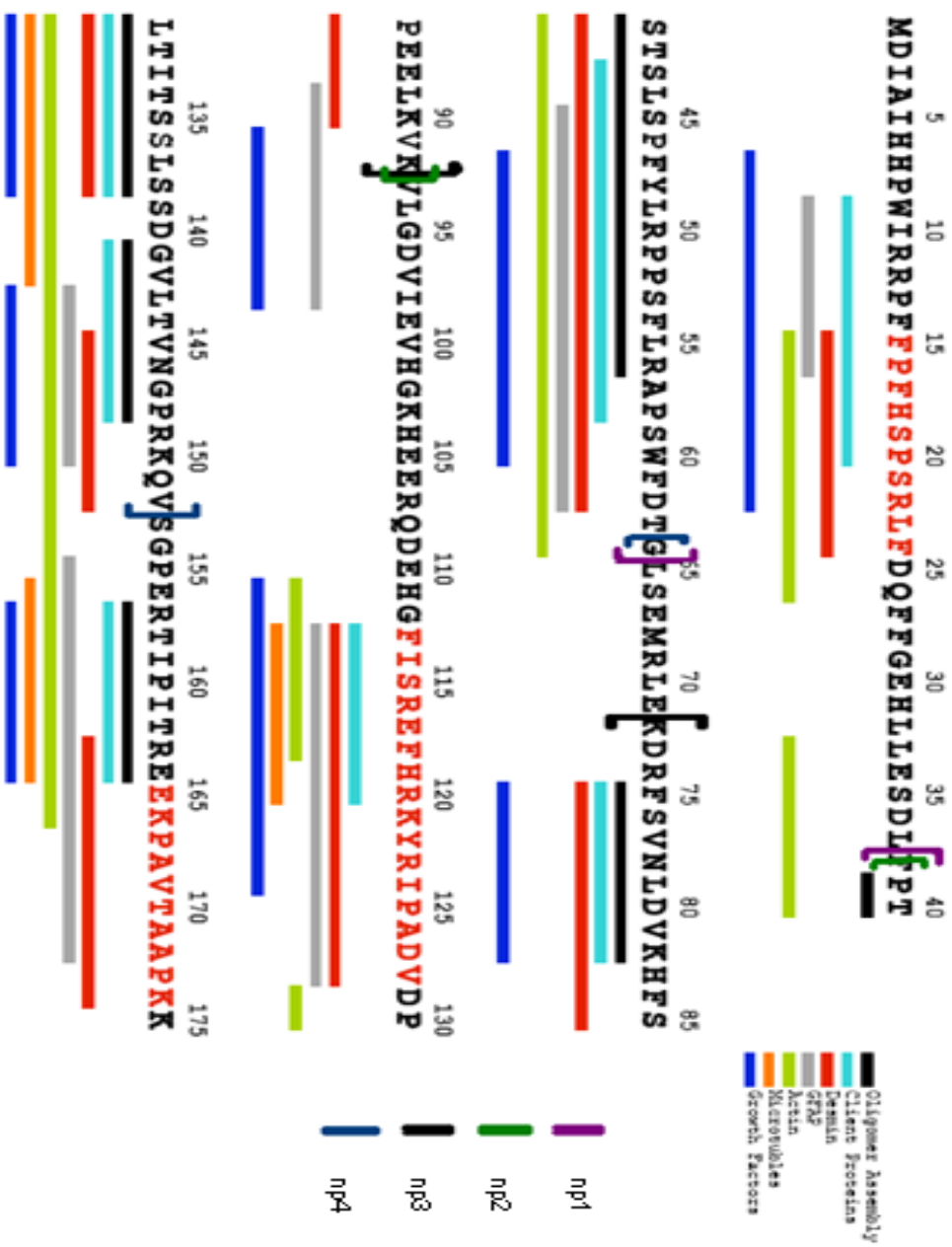

Figure 1.4 The αB-crystallin sites which will be included in the nanoparticles
The binding sites of several of the substrates of αB-crystallin are marked onto its amino acid sequence. The regions of αB-crystallin that will be used for the creation of four 'super chaperones' are shown on the sequence with square brackets. Np1 includes the regions 38-64, np2 is 38-92, np3 is 73-92 and np4 is 64-153. These regions were picked for the substrate binding sites which they contain. Adapted from a figure by Andrew Landsbury.

2. Materials and Methods

2.1. Chemicals

Unless stated otherwise, all chemicals and reagents were purchased from Sigma (UK) Fischer Scientific (UK)

2.2. Bioengineering of nanoparticle peptides

P6c-Mal-np plasmids encoding the nanoparticle peptide were a kind gift from Peter Burkhard. Three of the four αB-crystallin sequences to be inserted into the nanoparticle (np1, np2, np4) were ordered from Sigma Genosys. Np3 was created by annealing primers. αB-crystallin WT pcDNA3.1 (-) from Ming-Der Perng was used as a template. 1µl of each of the forward and reverse primers was combined with 48 µl annealing buffer (100mM potassium acetate 30mM HEPES, 2mM Magnesium acetate (AnalaR) adjusted to pH 7.4 with KOH). This was put into a PCR block (Hybaid MBS 0.2G), 95ºC for 4 minutes, then 70ºC for 10 minutes. This was cooled slowly to 4ºC. This primer was then phosphorylated: 2µl was added to 1µl of T4 PNK buffer and 5µl MQ water and 1µl 10mM fresh ATP (5mg/ml MQ water and disodium salt to a final concentration of 1mM). This was amplified; 37ºC for 30 minutes, 70ºC for 10 minutes and then 37ºC for a further 5 minutes. This was then allowed to cool to 4ºC.

This annealed oligonucleotide then had to be ligated into the p6c-Mal-np vector: 2µl was added to 1µl 10x ligase buffers, 1µl of p6c-Mal-np vector cut with $EcoR_1$ and SmaI restriction enzymes, 5µl MQ water and 1µl T4 DNA ligase. This kept at room temperature for 3 hours and then at 4ºC overnight.

The other 3 primers were amplified by PCR; 94ºC for 2.5 minutes, followed by 25 repeats of 94ºC for 30 seconds, a gradient of 56-68ºC for 30 seconds and 72ºC for 2 minutes, and finally flowed by 72ºC for 3 minutes. This was cooled to 4ºC. These were all cloned into the pGEM®-T-Easy vector (Promega) and then the p6c-Mal-np vector following the previous method.

2.3. Transformation of nanoparticle peptide plasmids

All 5 different p6c-Mal-np vectors and 50µl BL21 competent cells were thawed on ice. 1µl of the DNA was added to the cells and mixed very gently. The tube was incubated on ice for a further 30 minutes, and then heat shocked in a 42°C water bath for 45 seconds. It was then returned to the ice for 10 minutes, 250µl of sterile Luria Bertain (LB) (1% tryptone (Lab M), 0.5% bacto yeast extract (Becton, Dickinson and Company), 1% NaCl) was added and the mixture was incubated at 37°C for 1 hour in a bacterial shaker, 225 rpm. Meanwhile agar plates were prepared. Sterile agar (LB+ 1.5% agar (Melford)) was melted using a microwave, allowed to cool to 50°C, before 200mg/ml carbenicillin (Melford) and 30 mg/ml chloramphenicol were added. 25ml was poured onto each plate, and they were allowed to set. 20µl, 50µl and 200µl of the cells, now containing the plasmid, were spread onto 3 different plates, and they were left, upside-down, to incubate overnight at 37°C. They were then moved to 4°C to prevent further growth.

2.4. Expression of nanoparticle peptides

A pipette tip was used to pick a bacterial colony from the transformed plates, and was inoculated into 20ml of sterile LB, with 200mg/ml carbenicillin, 30 mg/ml chloramphenicol and 0.05% glucose (Merck), and grown overnight at 37°C at 225 rpm. 1L of sterile LB with the same additions was inoculated 1:100 with the overnight culture, and was grown at 37°C at 170rmp until $O.D_{600}$ had reached 0.5-0.6 (about 3 hours), measured with a DU640 spectrometer (Beckman). 0.5ml of the overnight culture was put in an Eppendorf tube with 0.5ml 80% glycerol to make a glycerol stock, which was stored at -80°C. Isopropyl-1-thio-β-D-galactopyranoside (ITPG) (Melford) was added to a final concentration of 1mM to induce expression of the nanoparticle peptides, and the culture was incubated for a further 3 hours. The culture was then harvested by centrifugation at 8,000rpm for 30 minutes at 4°C using a JlA-8.1000 rotor (Beckman) in a floor centrifuge (Beckman Coulter). The supernatant was discarded and the pellet was resuspended in 20ml lysis buffer (9M Urea, 100mM NaH_2PO_4 (BDH), 10mM Tris (Melford)) pH 8.0; this

was stored at -20°C until used. 1ml samples were removed from the culture before induction and before harvesting. These were centrifuged for 5 minutes at 13,200rpm using a benchtop centrifuge (IEC Micromax), the pellets were resuspended in 200µl 1x sample buffer (as described in (Laemmli 1970) and were boiled for 5 minutes at 95°C. 10 µl was run using 14% (w/v) sodium dodecyl sulphate-polyacrylamide gel electrophoresis (SDS-PAGE) to confirm that induction was successful.

2.5. Purification of nanoparticle peptides

Due to the fact that the nanoparticle peptides were designed to include a His-tag, their purification was relatively simple. The resuspended pellet was thawed, and returned to room temperature. The cells were solubilised by sonication, using a Soniprep 150 sonicator (MSE) at amplitude of 30 mincrons for 1 minute and centrifuged at 20,000g for 40mins at 22°C using a JA-20 rotor (Beckman). 1ml of His-Select Nickel Affinity Gel was washed twice with 5ml water and twice with 5ml lysis buffer, then added to the supernatant, and incubated overnight at 20°C with gentle shaking This allowed time for the nanoparticle peptides to bind to the His-tag beads. The mixture was transferred to a free standing 10ml column, and washed with 20ml lysis buffer, pH 7.5, by slow addition of 1ml steps. Fractions of 1.5ml were collected in Eppendorf tubes. The beads were then washed in the same way with 20ml washing buffer 1 (100mM PO_4, 9M Urea; pH 6.8), 20ml washing buffer 2 (20mM citrate, 9M Urea; pH 5.9) and 20ml washing buffer 3 (20mM citrate, 9M Urea; pH 4.5). The nanoparticle peptides were then eluted from the beads using 20ml elution buffer (lysis buffer with 1M imidazole; pH 8.0) and collected in 1ml fractions. The fractions were run using SDS-PAGE; fractions containing nanoparticle peptides were pooled and dialysed overnight, with gentle stirring, into refolding buffer (20mM Tris pH 7.5, 150mM NaCl, 8M Urea, cleaned by adding Amberlite (Merck) and vacuum filtration using 0.2µm cellulose nitrate membrane filters (Whatman)). The concentration of the nanoparticle peptides were then quantified using Pierce BCA (bicinchoninic acid) protein assay kit (Thermo Scientific), adjusted to 0.3mg/ml and stored in 0.5ml aliquots in Eppendorf tubes at -80°C. The beads were cleaned by washing

with 2 volumes of deionised water, 5 column volumes of 2% SDS (Biorad), and then 30% ethanol, as per the product information, and stored in 30% ethanol at 4°C for reuse.

2.6. Assembly of nanoparticles

Nanoparticles were assembled in accordance to (Schroeder, Graff et al. 2009) (Pimentel, Yan et al. 2009) with some slight modifications. They were thawed, diluted to 0.1 mg/ml and dialysed overnight with stirring in assembly buffer (20mM Tris pH 7.5, 150mM NaCl, 8M urea). They then underwent stepwise dialysis with decreasing concentrations: 6M, 4M, 2M, 1M until 0M, each either for 3h or overnight, with stirring. This was carried out at room temperature.

2.7. Expression of αB-crystallin

A Glycerol stock of BL21 cells containing αB-crystallin was a kind gift from Andrew Landsbury. As with the nanoparticle peptides (see section 2.4. Expression of nanoparticle peptides), 20ml of LB was inoculated with 2µl of the glycerol stock, along with 50mg/ml carbenicillin, 34 mg/ml chloramphenicol and 0.05% glucose, and the culture was grown overnight at 37°C at 225rpm. Again, 10ml of the inoculum was then added to 1L of LB and the bacteria was grown at 37°C, 170rpm, until it reached an $O.D_{600}$ of 0.5-0.6, this time however, it was then induced with ITPG to a final concentration of 0.5mM. It was grown for a further 3 hours, and then harvested in a similar way to before, although instead of using lysis buffer in which to resuspend the bacterial pellet, 20ml resuspension buffer was used (50mM Tris pH 8.0, 1mM EDTA, 100mM NaCl, 10mM $MgCl_2$ (BDH), with 1 x protease inhibitor tablet (Roche) and 0.2mM phenylmethanesulfonyl fluoride (PMSF) (Calbiochem), dissolved in 100% ethanol added just prior to use). Again, SDS-PAGE was used to ensure induction had occurred, and the resuspended bacterial pellet was stored at -20°C.

2.8. Purification of αB-crystallin

αB-crystallin is soluble in the bacterial pellet, and so a soluble protein extraction was used to begin the purification procedure. Firstly, three freeze-thaw cycles were carried out to break open the bacterial cells. Each time, the bacteria was frozen and then returned to room temperature. Storage of the bacteria at -20°C was the first freeze step. After this, and once it was back at room temperature, lysozyme was added to a final concentration of 0.25-1mg/ml to further break open the resuspended bacteria. It was mixed well with a dounce plunger. It was then shaken for 15 minutes, using a bacterial shaker, at 37°C, 70rpm. Next, the mixture was dounce homogenized on ice to complete the lysis of the bacteria. It was centrifuged for 15 minutes, using a JA-20 rotor, at 16,000rmp, and at room temperature. The cell debris and insoluble proteins were pelleted and discarded, while the supernatant was retrieved. Benzonase nuclease was added to a final concentration of 10units/ml, and the solution was well mixed, again with a dounce plunger. It was then incubated at room temperature, with gentle mixing, for 30 minutes, before 5% P.E.I was added to a 1000 x final dilution and the solution was incubated for a further 10 minutes, again with gentle mixing, this time on ice. It was again centrifuged using a JA-20 rotor, although the speed was 20,000rpm, the temperature 4°C and the length of time 20 minutes. This pelleted the DNA and RNA, which was discarded, and the supernatant, containing soluble proteins was kept. This concluded the extraction of αB-crystallin from the bacterial cells, but it then had to be purified using high performance liquid chromatography (HPLC), for which a smaller volume than 20ml was required. Therefore, the solution was then concentrated using an Amicon ultra centrifugal filter, MW 10,000kDa (Millipore) at 4,500 rpm, 4°C for 15 minutes (Jouan CR4-22 centrifuge), repeated until the volume was 5ml.

The first HPLC step used for αB-crystallin purification was running an anion exchange (TMAE) column (Hitachi Merck, L-4250 UV-Vis detector, L-6210 intelligent pump). Line A was put into buffer A (20mM Tris pH 7.4, 1mM $MgCl_2$, 1mM EDTA, 1mM Dithiothreitol (DTT) (Melford), 0.2mM PMSF, 0.2μm vacuum filtered) and the column was equilibrated overnight, with a pump speed of 2ml/min. The protein solution was dialysed overnight at 4°C with stirring, also into buffer A. Equilibration was

confirmed by comparing pH and UV reading of the column flow through with that of buffer A. Line B was then put into buffer B (buffer A + 1M NaCl, also 0.2 μm vacuum filtered), the protein solution was injected onto the column, and chromeleon software was used set the gradient. As αB-crystallin should not bind to the column, it should be eluted in the first 15 minutes. Therefore the column was set to stay at 100% buffer A for 20 minutes, increase to 100% buffer B between 20 and 40minutes and stay at 100% buffer B until 70 minutes. It ran at 1ml/min, and so 1ml fractions were collected (Biorad 2110 fraction collector) in Eppendorf tubes. SDS-PAGE was used to identify the fractions that contained αB-crystallin and these were pooled.

Next, the solution was further purified by size exclusion chromatography (SEC). The column was equilibrated overnight using SEC buffer A (20mM Tris pH 7.4, 100mM NaCl, 0.2 μm vacuum filtered), again using 2ml/min through column A. The solution was concentrated to 0.25ml, and once equilibration was confirmed, it was injected onto the column. 1ml fractions again were collected and SDS-PAGE was used to identify αB-crystallin. Those containing αB-crystallin, but not impurities, were pooled, and BCA was used to determine the concentration, it was adjusted using the SEC buffer, and aliquots at a range of volumes and concentrations were stored at -80°C.

Each time a column was used it was cleaned afterwards. First 0.5M NaOH was run through for 1 hour, at a speed of 2ml/min to wash out the buffers and to sanitise. Next MQ water (Millipore) was run through at 2ml/min, until the flow through had returned to pH 7.0 (determined using pH indicator strips (BDH)). Finally, column storage buffer (1M NaCl, 0.02% (v/v) sodium azide) was run through at 2ml/min for 1 hour. All buffers were 0.2 μm vacuum filtered. The machine was switched off, and all 3 lines were left in MQ water.

2.9. Expression of desmin

The glycerol stock of BL21 cells with the desmin plasmid was another gift from Andrew Landsbury. The expression of desmin was carried out in exactly the same way as αB-crystallin (see section 2.7. Expression of αB-crystallin).

2.10. Purification of desmin

As desmin is an insoluble protein, the first step of purification was an insoluble protein extraction. This begins in the same way as the soluble protein extraction (see section 2.8: Purification of αB-crystallin), since the same method is used to break open the bacterial cells. The resuspended pellet underwent three freeze-thaw cycles, and upon reaching room temperature, lysozyme was added to a final concentration of 0.25-1mg/ml. It was mixed well with a dounce plunger, shaken at 37°C for 15 minutes, homogenised and then centrifuged for 15 minutes, room temperature, 16,000rpm using a JA-20 rotor. This time, however, the pellet was saved and the supernatant was discarded. It was resuspended in 20ml buffer 1 (20mM Tris pH 7.4, 150mM NaCl, 5mM EDTA, 1mM EGTA, with 0.5mM DTT, 0.2mM PMSF and 1% v/v triton added prior to use), and this was homogenised. Benzonase nuclease was added to a final concentration of 10units/ml, was mixed well, and incubated for 30 minutes at room temperature with gentle mixing. It was then centrifuged again at 20,000rpm for 15 minutes, this time at 4°C. The supernatant was discarded and the pellet was resuspended in 20ml buffer 2 (20mM Tris pH 7.4, 150mM NaCl, 5mM EDTA, 1mM EGTA, with 0.5mM DTT, 0.2mM PMSF, 0.5% v/v triton and 1.5M KCl added prior to use), homogenised and mixed gently at room temperature for 15 minutes. After another centrifugation with the same conditions, the pellet was resuspended and homogenised in buffer 3 (20mM Tris pH 7.4, 150mM NaCl, 5mM EDTA, 1mM EGTA, with 0.5mM DTT and 0.2mM PMSF added prior to use), and again mixed gently for 15 minutes at room temperature. It was again centrifuged, and this time resuspended and homogenised in 5ml desmin TMAE buffer A (7M Urea, 10mM Tris pH 8.0, 1mM EDTA, 1mM DTT, 0.2mM PMSF, cleaned with amberlite and vacuum filtered. It was mixed gently at room temperature until the pellet had dissolved, and centrifuged at 30,000rpm for 30 minutes at 4°C using an MLA-80 rotor. It was then purified using a TMAE column, in the same way as described for αB-crystallin (see section 2.8. Purification of αB-crystallin), but using a linear gradient where % buffer B (buffer A + 1M NaCl) increases by 1%/min. The fractions containing desmin were again identified using SDS-PAGE, pooled the concentration was quantified using a BCA protein assay. The concentration was adjusted to 1mg/ml using TMAE buffer A and frozen in 1ml aliquots.

2.11. Citrate synthase chaperone assay

Citrate synthase purified from porcine heart was bought from Sigma. Before it can be used in a chaperone assay, it must be dialysed overnight at 4°C into CS buffer (50mM Tris pH 8.0, 2mM EDTA). Subsequently, it can be stored at 4°C. The protein concentrations of the citrate synthase and the chaperone (either assembled nanoparticles or αB-crystallin) were then quantified using a BCA assay. The concentration of citrate synthase was adjusted to 0.5mg/ml using CS buffer. The 6 micro cuvettes that are used for the assay were meanwhile cleaned by 30 minutes sonication (Branson 1510 sonicator) in 5% Teknon 100 detergent, rinsed and allowed to air-dry. For each of the chaperones, citrate synthase (the substrate) was used at a final concentration of 0.15mg/ml, and the chaperone was used at both a 2:1 and 20:1 substrate:chaperone ratios. The assay was carried out using the kinetics/time function on the DU640 spectrometer. For each cuvette, the sample was compiled: lane 1 was a negative control (only chaperone), lanes 2-4 were the chaperone assays (chaperone and substrate, three identical repeats), lane 5 was a positive control (only substrate) and lane 6 was a blank. The negative control contained an equivalent amount of chaperone buffer (either αB-crystallin SEC buffer or nanoparticle 0M Urea refolding buffer) to remove the possibility that any chaperone effect seen is due to the buffer present. Each sample was made up 220µl using CS buffer. The machine was set to 44°C and allowed to reach full temperature before the assay was begun. The cuvettes were not pre-warmed. All 6 cuvettes were then loaded with the sample, tapped and wiped to remove air bubbles and smears, and inserted into the machine. It was run for 30 minutes, taking readings every 15 seconds at OD_{360}. The cuvettes were rinsed and allowed to air-dry between each assay. Each of the four conditions was repeated three times, each time with separately prepared citrate synthase and separately assembled nanoparticles.

2.12. γ-crystallin chaperone assay

γ-crystallin, purified from bovine lens' was a kind gift from Frederique Tholozan, in a buffer of: 2mM EGTA, 1Mm $MgCl_2$, 1mM DTT. This assay was only used for nanoparticles, and not for αB-crystallin, due to the high temperature needed. The method was as for the citrate synthase chaperone assay (section 2.11, citrate synthase chaperone assay), apart from the following two differences: the samples were made up to 220µl using 0M Urea folding buffer and the assay was run at 70°C.

2.13. Desmin assembly and sedimentation assay

The concentrations of desmin, αB-crystallin and assembled nanoparticles were requantifed using a BCA assay. 300µl samples were compiled using 0.5mg/ml desmin at a ratio of 1:1 with chaperone, made up to volume using desmin TMAE buffer A. Controls of each of the three proteins by themselves were also made, and each of the five samples was repeated three times. They were all dialysed overnight in desmin assembly buffer (20mM Tris pH 8.0, 1mM DTT, 1mM EDTA, 4M Urea, cleaned with amberlite and vacuum filtered) at room temperature. They then underwent stepwise dialysis with decreasing concentrations of Urea (2M, 0M) each for 3 hours at room temperature. The samples were then transferred into the final assembly buffer (20mM tris pH 7.0, 50mM NaCl) for overnight dialysis, one of each of the five samples were put at 22°C (room temperature), 37°C (37°C room) and 44°C (oven).

The next day, the results were processed using a sedimentation assay. They were removed from their dialysis bags, and 50µl of each of the 15 samples were centrifuged in Eppendorf tubes at for 10 minutes at low speed (2,450g) at room temperature using a benchtop centrifuge (Eppendorf 5417R). 50µl was also centrifuged on a 0.85M sucrose cushion for 30 minutes at high speed (30,000rpm), using a TLS-55 swing rotor (Beckman) in a Beckman Coulter optima max ultracentrifuge, at room temperature. For both centrifugations, the supernatant was removed carefully from the pellet, and the pellet was redissolved in 150µl 1x sample buffer. All of the protein present in the supernatant was

precipitated using methanol-chloroform precipitation (see section 2.14. Methanol-chloroform precipitation), and also redissolved in 150µl 1x sample buffer. All 60 samples were boiled for 5 minutes at 95°C, and 10µl of each was run on a 14% gel using SDS-PAGE. Once they had been run, the gels were fixed for 20 minutes using fixer solution (50% methanol, 10% acetic acid), stained for 25 minutes using comassie blue (50% v/v methanol, 10% v/v acetic acid, 0.25% w/v Coomassie brilliant blue R-250(Biochemical)) and then destained using destain solution (10% methanol, 5% acetic acid) until the bands were clear enough for quantification. The gels were photographed using Fujifilm intelligent darkroom technology and image gauge software was used to quantify the band intensity, and hence the amount of protein, on the gels. This experiment was repeated four times, each time with newly assembled nanoparticles and with a new set of desmin buffers.

2.14. Methanol-chloroform precipitation

Methanol-chloroform precipitation was used to precipitate any protein present in the supernatant after the sedimentation assays. To the sample, 4x sample volume of methanol, 1x sample volume of chloroform and 3x sample volume of water were added. This was vortexed, and then centrifuged at 12,000rpm for 5 minutes in a benchtop centrifuge. The top layer was discarded, and 3x sample volume of methanol was added. The sample was again vortexed and centrifuged in exactly the same way. The supernatant was discarded, leaving the precipitated protein.

2.15. Preparation for TEM

To prepare grids for use in the transmission electron microscope, mica coated in carbon was dipped into an Eppendorf lid containing 345µl buffer and 5µ sample. It was then put into 1% uranyl acetate (AnalaR). The carbon was lifted from underneath onto a 3.05mm copper grid (Agar), and then used in the TEM.

3. Results

3.1. Bioengineering, expression and purification of the nanoparticle peptides

The plasmid p6c-Mal-np encoding the engineered nanoparticle (Schroeder, Graff et al. 2009) (Pimentel, Yan et al. 2009) was transformed directly into BL21 cells. It was also spliced and ligated to include a region of αB-crystallin DNA before transformation. Four different nanoparticles were created that were designed to contain regions from αB-crystallin important in binding client proteins. These expression vectors were p6c-Mal-np1 (containing region 38-64 of the amino acid sequence), p6c-Mal-np2 (38-92), p6c-Mal-np3 (73-92) and p6c-Mal-np4 (64-152) (Figure 1.4). The transformed cells were cultured and induced to express the nanoparticle peptides (Figure 3.1A, tracks 1 and 2). These pre- and post-induction samples show clearly that that the addition of ITPG led to the production of a protein with a molecular weight of about 14 kDa (arrow). Given that the nanoparticle peptides should have a calculated molecular weight of 12.5 kDa, it can be assumed that the induced protein was in fact the nanoparticle peptide. A large quantity of the protein was produced in comparison to the host proteins, so this is clearly a very efficient expression vector.

The nanoparticles were purified by affinity chromatography using the bioengineered his-tag and a nickel affinity column. The elution fractions (Figure 3.1A, tracks 6-10) of the nanoparticle peptides show two bands, one at 14 kDa (arrow), which is assumed to be the monomer, and another at 43 kDa (double arrow). This is a major band; however it cannot be seen in any of the other lanes. Therefore it can be concluded that this band is from a protein which was not present in that form during the culturing and harvesting of the bacteria. The molecular weight of this band is about three times that of the monomer, thus it is likely that the band represents a trimeric form of nanoparticle peptide, which was previously prevented from oligomerisation by bacterial factors. Although proteins usually retain little secondary structure in SDS, the monomers contain trimeric coiled-coil oligomerisation domains, and it has previously been seen that trimeric coiled-coils can be SDS-resistant (Chen, Lu et al. 2010) (Hayashi, Yamasaki et al. 1995). More structural investigations would be needed to confirm this.

The gels of the purification of the other nanoparticles (Figure 3.1B) do not differ from the ‘empty’ nanoparticles; the αB-crystallin did not appear to affect the process.

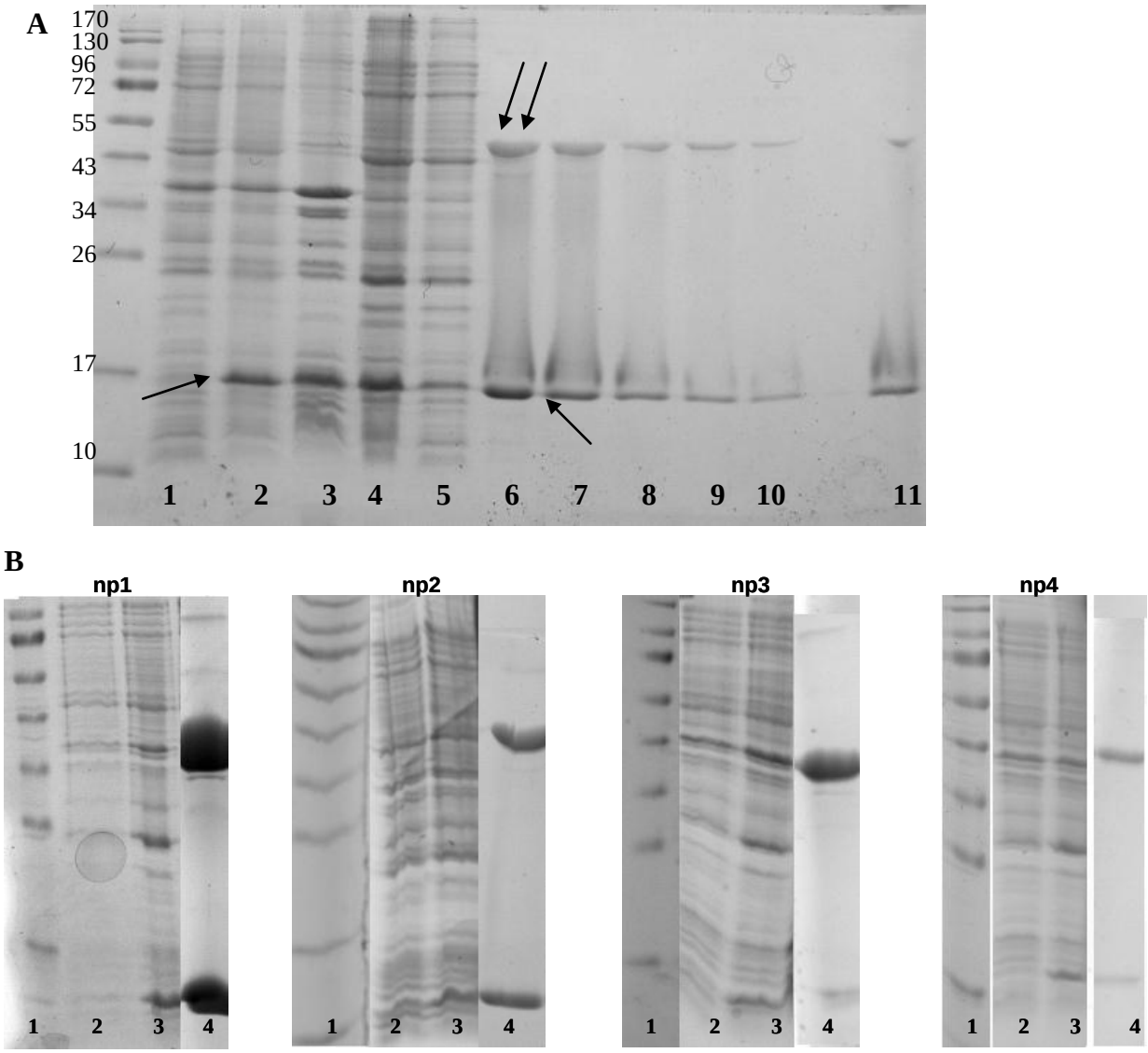

Figure 3.1 Nanoparticle peptide expression and purification gel (SDS-PAGE)
A E.coli BL21 were transformed with the plasmid p6c-Mal-np and protein expression induced by the addition of IPTG. Comparing a sample of the pre-induction culture (track 1) with a sample from an IPTG induced culture (track 2) shows the expression of one additional band (arrow) corresponding to the nanoparticle. Once sonicated and centrifuged, the nanoparticle was present both in the supernatant (track 3) and the pellet (track 4) indicating that not all of the cells had been lysed. The supernatant was incubated with his-beads and put onto the column; the lack of nanoparticle in the flow-through (track 5) shows binding to the beads was efficient. After washing, the nanoparticles were eluted (tracks 6-10) and fractions containing nanoparticles (fractions 1-7) were pooled (track 11); these were very clean. The protein ladder is on the right, with associated weights labelled in kDa.
B Reduced gels of the other four nanoparticles showing ladder (track 1), pre-induction (track 2), post-induction (track 3) and purified nanoparticle (track 4). All show the same features as in A.

3.2. Assembly of the nanoparticles

3.2.1. Assembly of 'empty nanoparticle'

Once purified, the nanoparticle peptides were assembled. From computer modelling, they should self assemble to form 60-mers, with a diameter of 16nm. However, it was previously found that in practice the amount of monomers varied, and was affected by buffer conditions and concentration. At the conditions used here the average number of monomers was 44, determined by analytical ultracentrifugation, and the diameter was 16nm, determined by electron microscopy (Raman, Machaidze et al. 2006).

The design of the nanoparticles lent itself particularly well to their assembly; after stepwise dialysis into a 0M urea buffer they should self-assemble. Following successful assembly, highly symmetrical spherical nanoparticles should form; this was verified with TEM. Figure 3.2A shows that nanoparticles did indeed form. Most of the nanoparticles were in the shape of a regular sphere, although there was some variation, and the size varied between 15-22 nm.

One interesting finding was that when run on a SDS-PAGE gel, these assembled nanoparticles did not produce a band. Upon closer inspection, there was found to be staining between the stacking gel and the resolving gel, indicating a protein that was too big to enter the resolving gel. As the molecular weight of the monomer was 12.5 kDa, the molecular weight of a 60-mer would therefore be 750 kDa, certainly too large to run onto the gel. It is likely that, again, the trimeric coiled-coils were resisting SDS solubilisation; the design of the nanoparticle would mean that if this is the case the structure would remain as a whole.

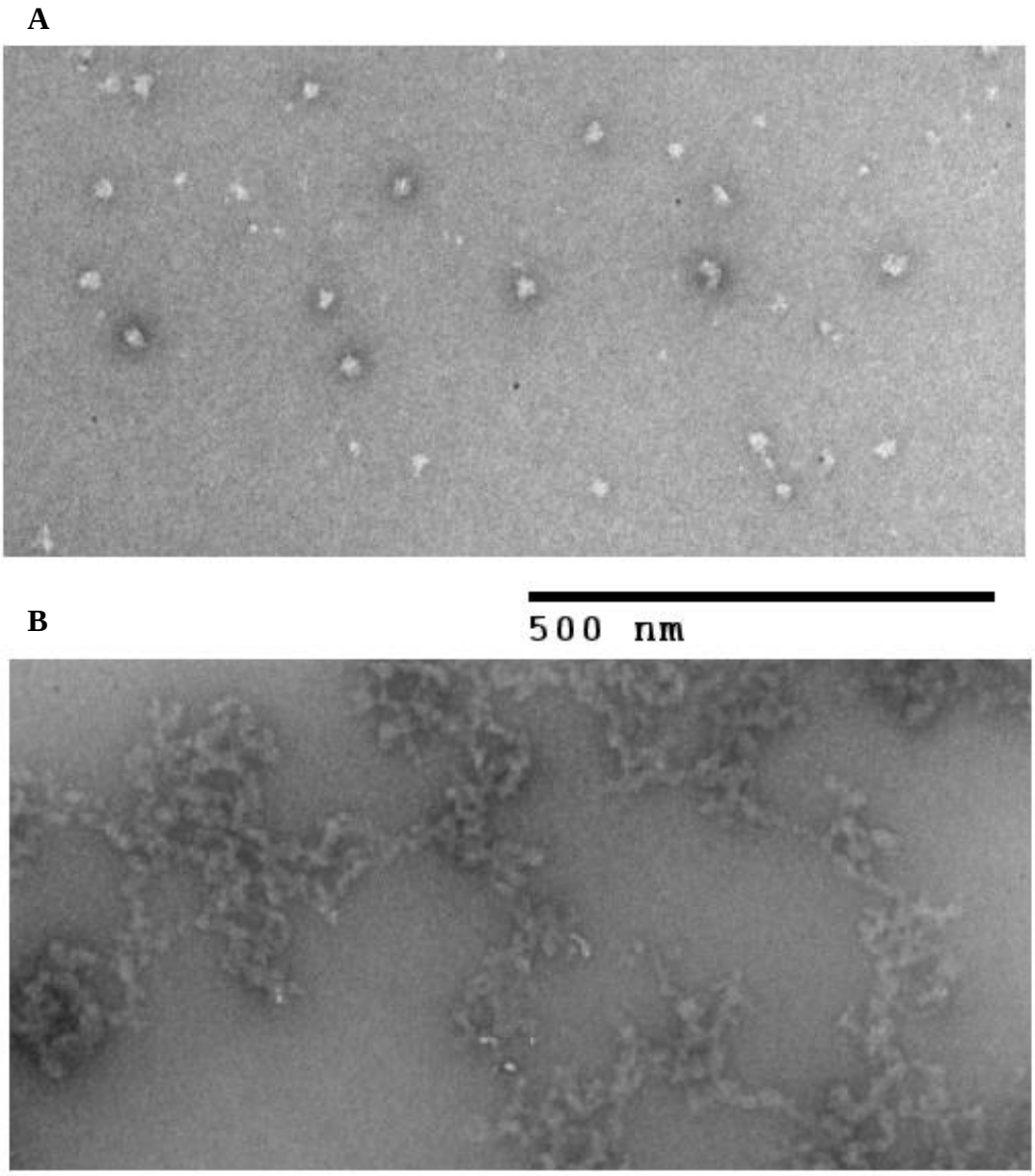

Figure 3.2 TEM image of assembled nanoparticles
A. Assembled 'empty' nanoparticles - np
B. Aggregated nanoparticle peptides containing αB-crystallin region – np1. This is representative of all four different αB-crystallin containing nanoparticles.
Both taken at 60000x magnification and stained with 1% uranyl acetate

3.2.2. Assembly of nanoparticles displaying regions of αB-crystallin

The nanoparticles containing αB-crystallin regions were assembled in the same way as those without. Again they were expected to form spheres, with the αB-crystallin regions displayed on their surfaces. It was unknown whether the addition of the regions would effect the number of monomers in a nanoparticle; the addition of a region of the SARS virus to the monomer led to particles of 110 monomers being formed (Pimentel, Yan et al. 2009)

However, upon dialysis out of urea all four of the samples produced a visible white precipitate that was not seen for np. This suggested that the nanoparticle peptides had aggregated instead of forming spheres. This was verified for one of the samples, np2 by TEM (Figure 3.2B).

3.3. Chaperone assays

As the nanoparticles containing αB-crystallin regions did not form, only the 'empty' nanoparticle, np, was used in the chaperone assays. To test for chaperone function; that is, the ability to stop non-native proteins from aggregating, three assays were used. In the first two, the client protein was put under denaturing conditions, in which it would ordinarily aggregate, both with and without nanoparticles present. Chaperone function would be indicated by the nanoparticles preventing aggregation of the client proteins. The two assays were carried out at very different temperatures to investigate the temperature range of activity. The third assay, on desmin filaments, was different, instead of denaturing the substrate, the assay tested effect of the chaperone on filament-filament interactions; by preventing them it would prevent aggregation.

Being the archetypal sHSP (small heat shock protein), and thus the natural small chaperone about which most is known, αB-crystallin was used as a control.

3.3.1. Citrate synthase chaperone assay

In the citrate synthase chaperone assay, a temperature of 44°C was used to cause denaturation of the citrate synthase. As the protein unfolds and aggregates, it causes the beam of light that passes through the cuvette to scatter, producing a higher OD. Therefore, with successful chaperoning, a lower OD is observed. The results of this assay

A

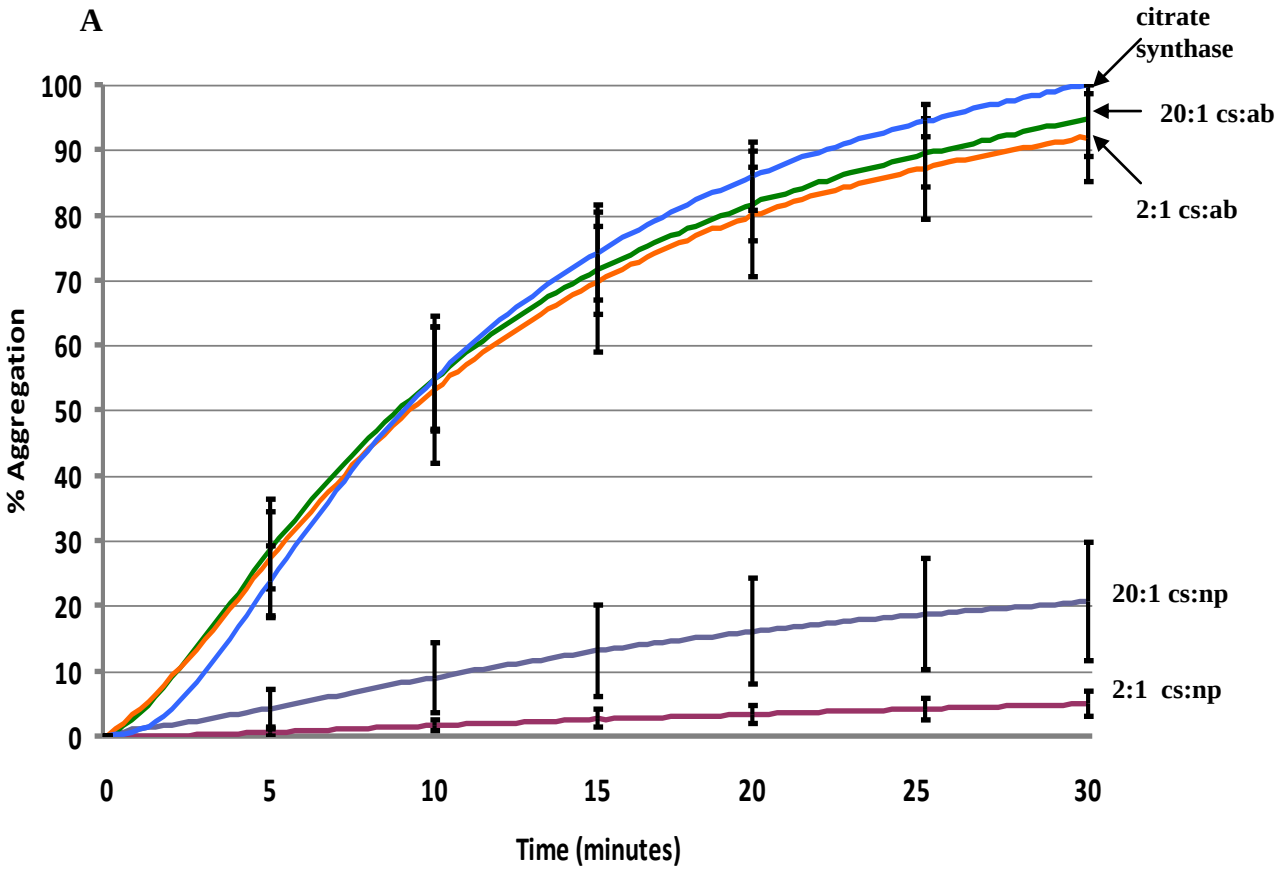

B

chaperone, CS:chaperone	%aggregation
np, 1:20	20.6 ± 9.0
np, 1:2	4.9 ± 1.9
ab, 1:20	94.8 ± 5.8
ab, 1:2	91.9 ± 6.8

Figure 3.3 Results of the citrate synthase chaperone assays
A) Graph of % citrate synthase aggregation over time, as indicated by optical density (OD). CS stands for citrate cynthase, ab for αB-crystallin and np for nanoparticle. Data points show the mean result of nine repeats, and error bars represent one S.D. in each direction.
B) Table of final % aggregation after 30 minutes, relative to citrate synthase control.

are shown graphically in Figure 3.3, where the level of aggregation in the presence of each chaperone is compared to a positive control where the aggregation of citrate synthase is measured in the absence of a chaperone protein (Figure 3.3A). The percentage aggregation after the full 30 minutes relative to control is also shown (Figure 3.3B). Both of the chaperones were tested at a substrate-to-chaperone ratio of 2:1 and 20:1, and each assay was carried out in three sets of three (nine repeats). The graph shows how remarkable the chaperone function of the nanoparticles was in this assay: at a ratio of 2:1 there was virtually no aggregation, indicating complete chaperoning. The result for the assay using αB-crystallin at the same concentration, however, was much more modest, with a final level of aggregation of 91.9%. A lower value would be more expected, but nothing close to 4.9% (Hayes, Devlin et al. 2008) (Ghosh, Estrada et al. 2005). The low level of αB-crystallin chaperoning could be due to error with protein concentration quantification, however the concentrations of both αB-crystallin and the nanoparticles were quantified in the same assay, and thus both would be subject to the same error. This makes the results for the nanoparticles particularly impressive.

Whilst the result for the 2:1 assay were remarkable, the results for the 20:1 assay were, in some respects, even more so. In this instance, there was a very small amount of chaperone relative to substrate, yet an impressive degree of chaperoning was still observed, with the final aggregation level only 20%. Again chaperoning at this low level would not be expected for sHSPs; the result for αB-crystallin at the same ratio of aggregation of 94.8% ± 5.8, indicating virtually no chaperoning at all, is unsurprising. This high level of chaperoning for what is a relatively small concentration of protein suggests that the nanoparticles chaperone not only well, but also by a very efficient means.

3.3.2. γ-crystallin chaperone assay

The unfolding of γ-crystallin in this chaperone assay was again temperature induced, however in this instance a much higher temperature of 70°C, was used to denature the substrate. At this temperature αB-crystallin formed flocculate aggreagates, so no sHSP was used as a control. The results (Figure 3.4) are very similar to those for the citrate

synthase assay. Again, the nanoparticles showed a very high level of chaperone function, with a final aggregation of 9.1% for a substrate-to-chaperone ratio of 2:1 and 23.9% for 20:1. This is further evidence that these nanoparticles function both well and efficiently as protein chaperones.

A

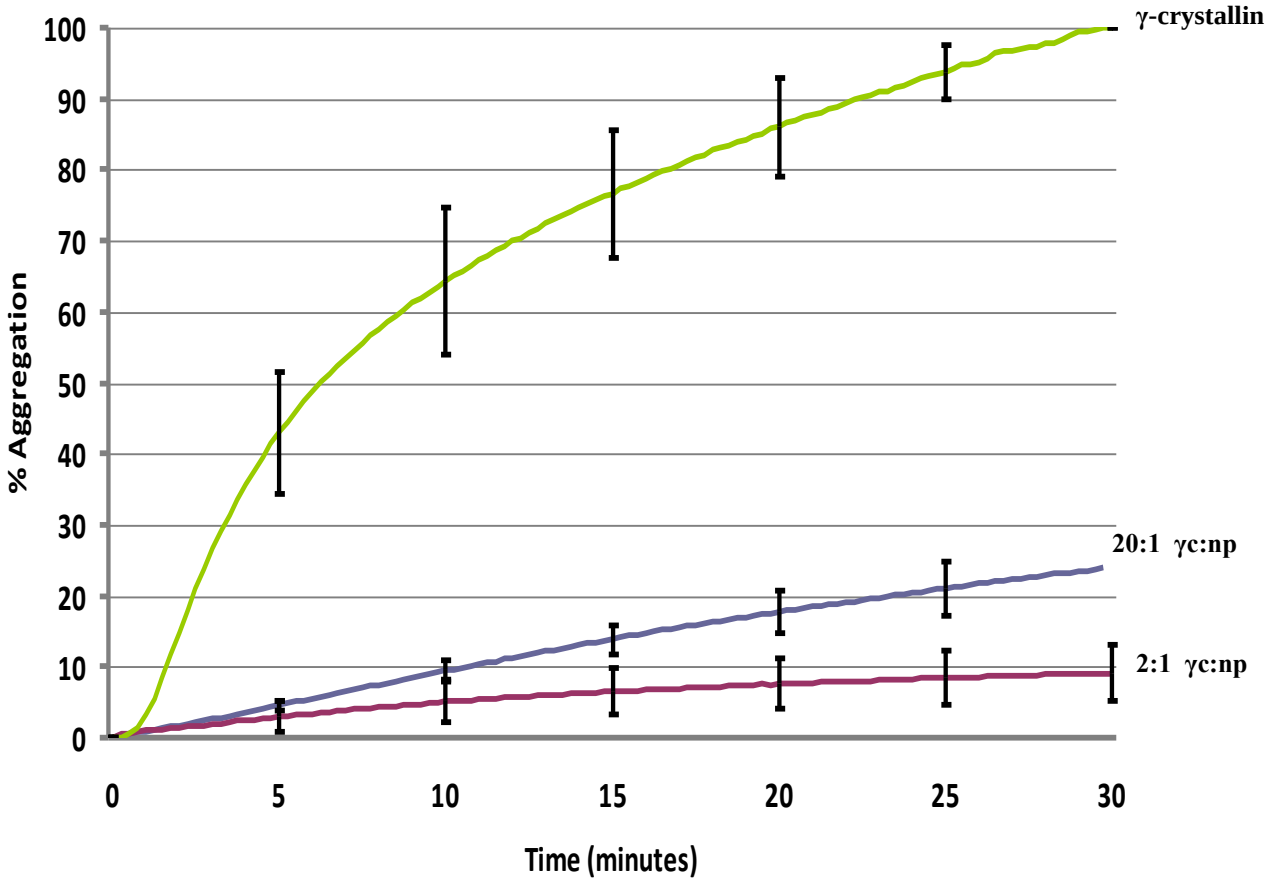

B

γ-crystallin : np	% aggregation
1:20	23.9 ± 4.4
1:2	9.1 ± 4.0

Figure 3.4 Results of the γ-crystallin chaperone assays
A) Graph of % γ-crystallin aggregation over time, as indicated by optical density (OD). γc stands for γ-crystallin and np for nanoparticle. Data points show the mean result of nine repeats, and error bars represent one S.D. in each direction.
B) Table of final % aggregation after 30 minutes, relative to γ-crystallin control.

The results also show the stability of the nanoparticles. At 70°C, a temperature at which most proteins would become denatured, they have not lost any functionality. This again illustrates how strong the interactions that hold the nanoparticles together are.

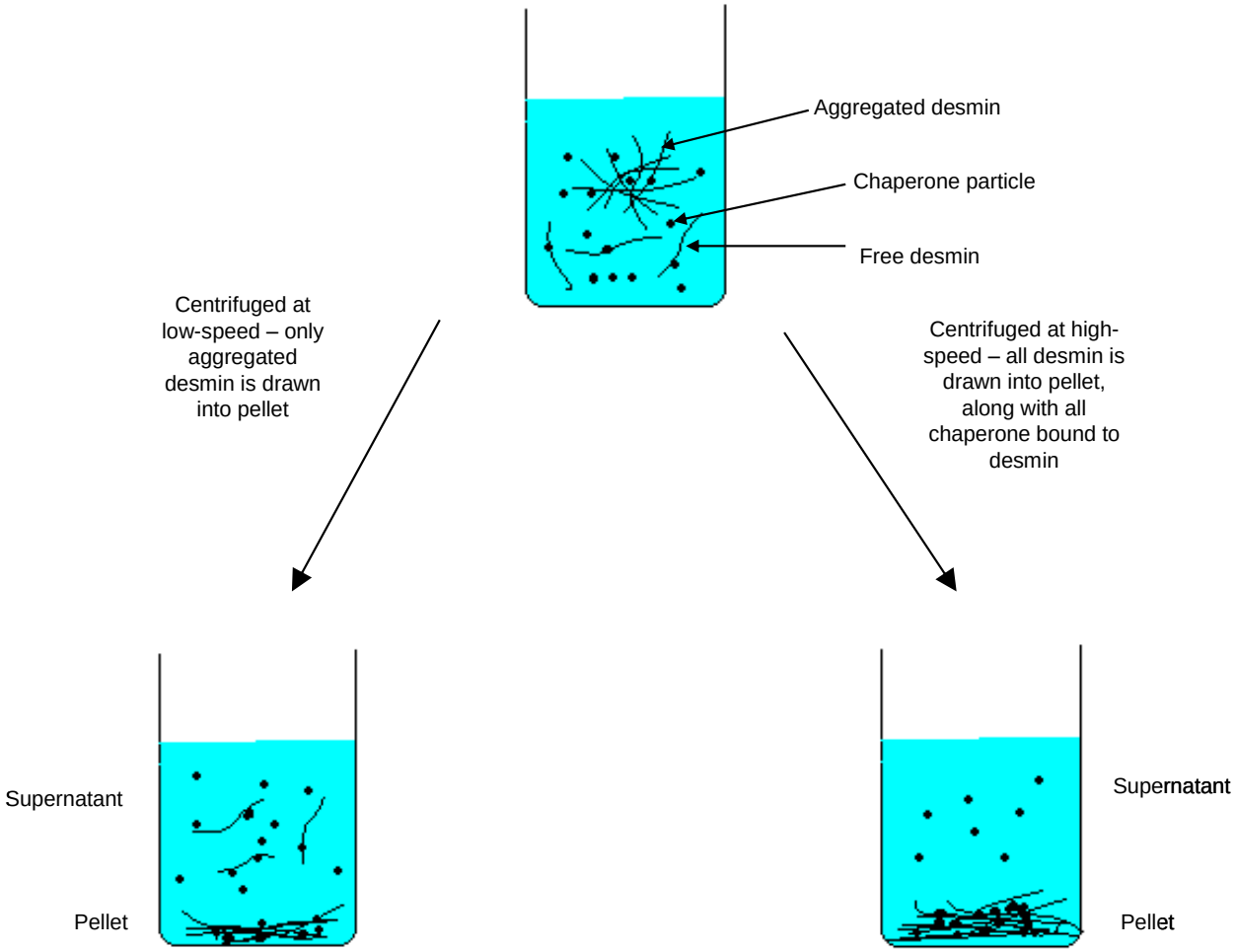

Figure 3.5 Diagram to summarise low and high speed sedimentation assays
When centrifuged at a low speed, only aggregated desmin will be found in the pellet, and so the more desmin in the supernatant, the less has aggregated and the better the chaperone. Under high speed centrifugation all desmin will be drawn into the pellet, regardless of its aggregation state, and any chaperone bound to desmin will be pulled into the pellet too. Therefore, the more chaperone found in the pellet, the higher the level of chaperone binding.

3.3.3. Desmin assembly chaperone assay

This chaperone assay differs from the previous two; the client is not unfolded, instead filament-filament interactions are promoted. Desmin is prepared for assembly by a

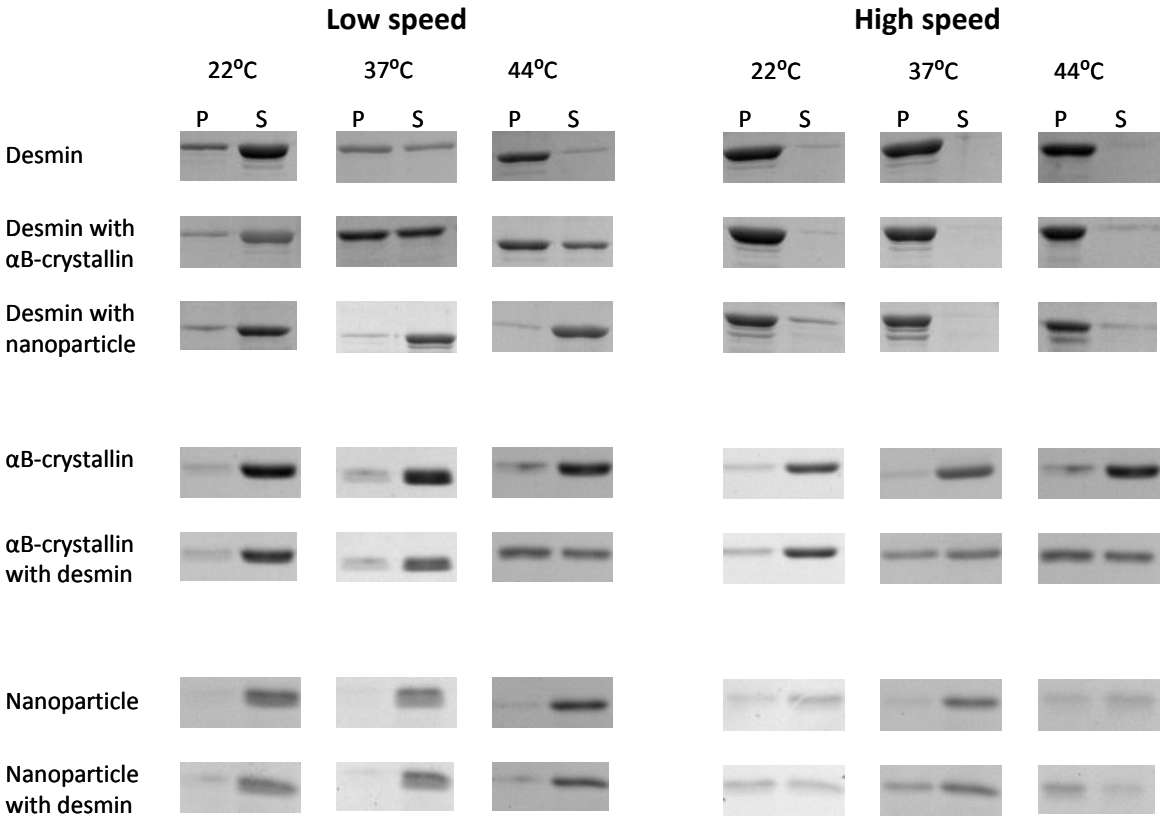

Figure 3.6. Gels from the desmin assembly sedimentation assay.
Samples were spun at both a low speed and a high speed. The supernatants were precipitated using methanol-chloroform, and then resuspended in 1 x sample buffer. The Pellets were also resuspended in the same volume of 1 x sample buffer. Samples were run on 14% SDS-PAGE gels. P indicates pellet and S indicates supernatant. The experiment was repeated four times: one example for each protein in each sample is shown for low and high speed, and at each of the three temperatures. The density of the bands was measured using image gauge software, from which a bar chart was created to show the percentage of protein in the pellet for each sample.

sequential dialysis strategy. It is then assembled into filaments at three different temperatures - 22°C, 37°C and 44°C - as the higher the temperature, the higher the level of filament-filament interactions; the assay measures the chaperone's ability to prevent these interactions. The process is carried out with desmin alone and in the presence of each chaperone. They also both underwent the assay without desmin as controls. The level of aggregation is determined by a sedimentation assay (summarised in Figure 3.5).

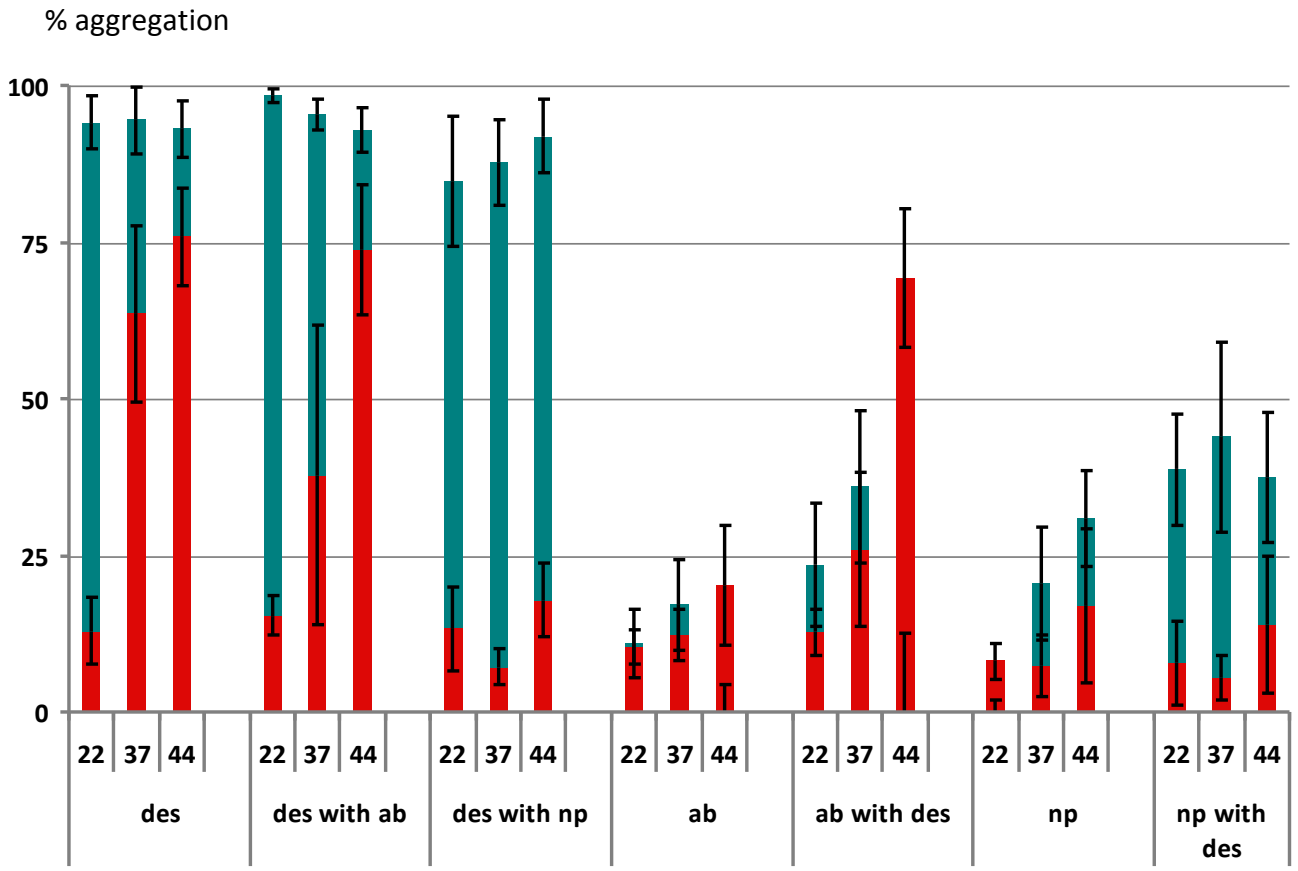

Figure 3.7 Graph of low speed and high speed sedimentation assays for desmin assembly chaperone assay
Bars correspond to the % of the protein found in the pellet out of the total amount of the protein in the sample. Red bars represent the low speed centrifugation (chaperone assay), and blue bars the high speed (binding assay). 22, 37 and 44 refer to the temperature at which assembly took place, in °C. Des stands for desmin, ab for αB-crystallin and np for nanoparticles. Data points are the average of four repeats. Anomalies were removed. Error bars are one S.D from the average in each direction.

Post-assembly, the samples are centrifuged at a low speed. Any aggregated filaments will be drawn down into the pellet, whereas unaggregated filaments will remain in the supernatant. Therefore, the more chaperoning that occurs, the higher the proportion of desmin left in the supernatant. The pellet and supernatant are then both run using SDS-PAGE (Figure 3.6) and the density of the bands is determined using image gauge software, enabling comparison of the amount of protein in the pellet against the amount in the supernatant (Figure 3.7). As previously discovered (see section 3.2. Assembly of the nanoparticles), the nanoparticles do not run well on the gel. However, it was found that a better result was obtained if they were first precipitated and then resuspended in sample buffer. This could be because the organic solvent is hydrophobic. Coiled-coils are thermodynamically driven to form their secondary structure because it shields their hydrophobic residues from the aqueous environment (Crick 1953). When in an organic solvent, however it is the hydrophilic and charged residues that are incompatible and this could drive the loss of the secondary structure. The precipitation procedure would then pellet the nanoparticles, and resuspension in SDS would mean the coiled-coils would not have a chance to reform.

Accordingly, the protein in all supernatant samples was precipitated using the methanol-chloroform precipitation method. Pellet samples were resuspended in sample buffer. This did allow nanoparticle bands to be seen, but it is worth noting that the presence of a small amount of dye at the top of the resolving gel indicates that not all of the nanoparticles were denatured by this method. This can be seen in Figure 3.6 where the density of nanoparticle bands visible in the gel is less consistent than the density visible for either desmin or αB-crystallin. Consequently, while an approximate ratio of the amounts of nanoparticles in the pellet and supernatant can be determined, accuracy is lacked. However, this does not affect the chaperone assays, where it is the proportions of desmin and not of chaperone that are examined. It is also worth noting that no trimer band was seen. This is in contrast to what was seen earlier (section 3.1.Bioengineering, expression and purification of the nanoparticle peptides), when trimers, as well as monomers were seen pre-assembly. This suggests that the suspension in SDS prevented any secondary structure from forming.

The samples also underwent centrifugation at high speed in order to establish chaperone binding to the desmin filaments (Figure 3.5). This speed causes all of the desmin to be drawn into the pellet, regardless of whether the filaments are interacting or not. Any protein that is bound to the filaments will therefore also be drawn into the pellet; hence, the more chaperone present in the pellet, the more has bound to desmin.

All of the samples were also examined using TEM (Figure 3.8). This was to see whether the desmin had formed filaments, and to examine their morphology. It should be noted that the TEM images do not give a reliable indication of aggregation, as images were selected that best showed the morphology of the filaments, and not the aggregates. Moreover, aggregated proteins tend to stain badly or break through the carbon during sample preparation and so often cannot be seen well. TEM can, in addition, give some indication of the level of chaperone binding.

The results of the high and low speed centrifugations are shown in the bar chart in Figure 3.7. At 22°C there was very little aggregation of desmin on its own, as shown by the red bar: only about 10% of the desmin was present in the pellet. This was as expected, but indicates there was nothing to chaperone; so it is unsurprising that the corresponding bars for αB-crystallin and nanoparticles are of the same height. The TEM images (Figure 3.8: G, J, M) show that for all three samples long, regular filaments were formed and so aggregation seems not to be occurring. At 37°C, however, about 60% of the desmin was present in the pellet, clearly showing that temperature was sufficient to cause the filaments to interact with each other and to aggregate, even though this aggregation is not apparent in the TEM image (Figure 3.8, H), for reasons discussed previously. What the image does show, however, is that the desmin formed normal filaments, and hence that it was the heat causing their aggregation and nothing else. The αB-crystallin chaperoned the aggregation to an extent, with about 40% of the desmin left in the pellet. The nanoparticles, however, again chaperoned to an incredible extent, leaving less than 10% of the desmin in the pellet: the desmin was almost completely chaperoned by them. They therefore, again, chaperoned at a much higher level then the sHSP.

What is even more impressive, though, is the result at 44°C. This high temperature caused 75% of the desmin to be brought into the pellet. Thermal stress at this level is too great for αB-crystallin, and consequently no chaperoning was seen. The

Figure 3.9 TEM images of the desmin assembly chaperone assay
Proteins were stained with 1% uranyl acetate and photographed at 80000x magnification. Images chosen are, where possible, representative of the filaments seen in the sample. The assay was undertaken to determine the effects of the two protein chaperones on desmin filament aggregation at three temperatures, 22°C, 37°C and 44°C. Samples containing only αB-crystallin, nanoparticles or desmin were used as controls.

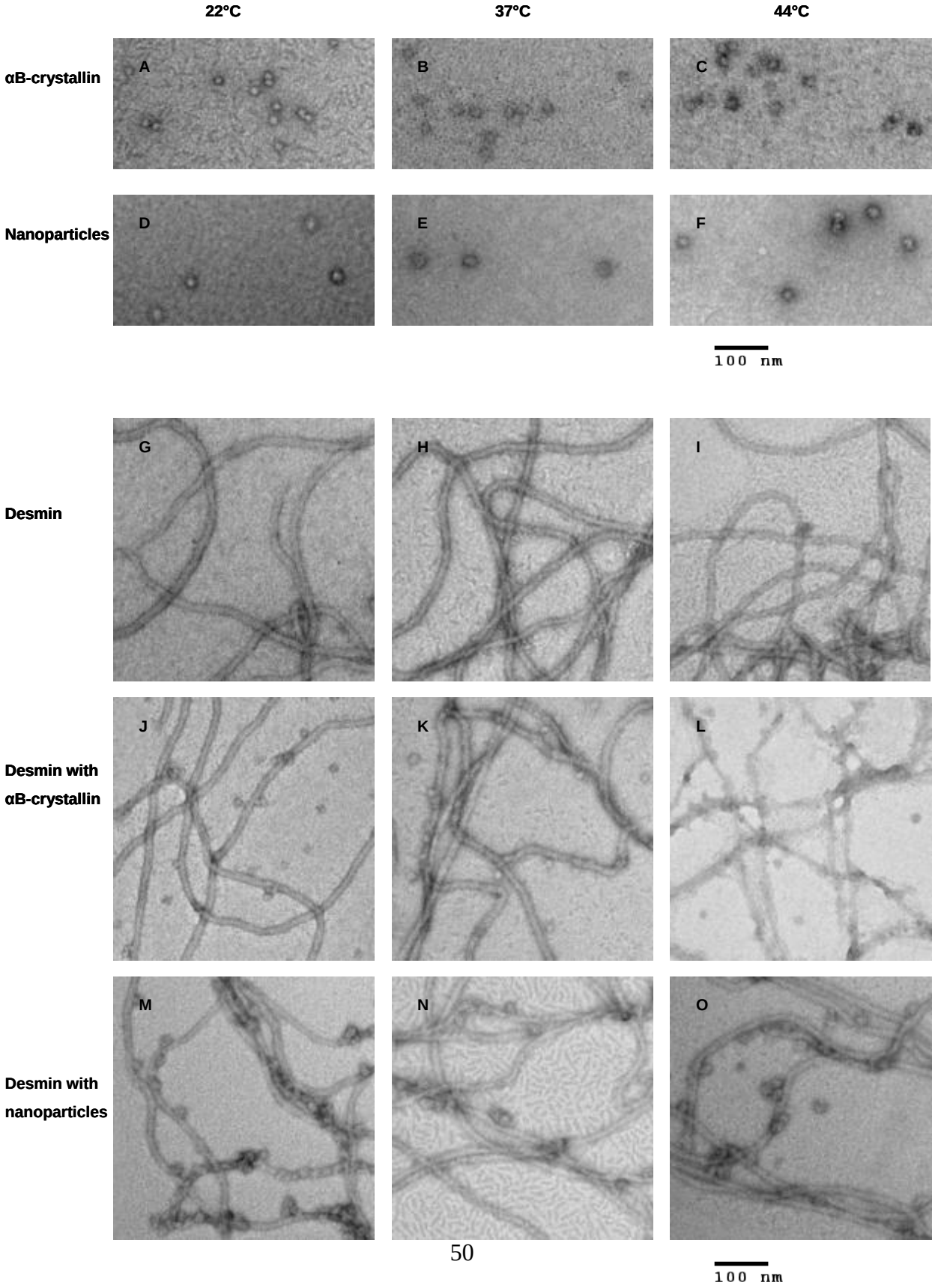

nanoparticles, however, still managed to chaperone the filaments, so that only 20% were aggregated enough to be in the pellet. For a temperature at which the natural chaperone had no effect at all, this really is a very exciting result.

Although the TEM images are not used for determining aggregation, what was telling was the ease of taking the 44°C image for the sample of nanoparticles with desmin (Figure 3.8, O) compared to desmin alone and with αB-crystallin. There were no fewer normal filaments seen on the grid than at lower temperatures. For desmin and desmin with αB-crystallin, though, it was difficult to find filaments on the grid that were not in aggregates (Figure 3.8, I and L). This is testament to the level of aggregation in these samples, and to the lack of it in the presence of nanoparticles.

The TEM was also used to ensure that the structures of neither of the protein chaperones were affected by the heat, which could be cause of a lack of chaperoning. However, the structures of both seem consistent throughout (Figure 3.8, A-F).

The high speed centrifugation (Figure 3.7, blue bars) was used to determine protein binding: the more of the chaperone that is present in the pellet, the more binding has occurred. For αB-crystallin with desmin, a small amount of temperature dependent binding is seen, as compared to αB-crystallin by itself, where, as expected, there is very little in the pellet. This is presumably because as the desmin is put under more thermal stress and so aggregates more, the αB-crystallin tries harder to chaperone it. These results are mirrored in the TEM images (Figure 3.8): at 22°C (J) binding cannot be seen, whereas at 37°C (K) and 44°C (L) it can.

The binding of the nanoparticles to desmin, however, seems to be temperature independent: between 35%-45% consistently remained in the pellet. Again, this result is mirrored in the TEM images: a large amount of nanoparticle binding is seen, regardless of the temperature (M, N, O). This binding reaction seems to be independent of chaperoning, as binding occurs when chaperoning is not needed. Furthermore, as the level of chaperoning increasing, the rate of binding stays the same. Although 35%-45% does not seem to indicate a high level of binding, its temperature independency implies that the nanoparticles could be binding to the desmin at capacity. This could be investigated by using a smaller concentration of nanoparticles relative to desmin.

4. Discussion

This project produced very exciting results: a new nanoparticle chaperone was found with remarkable chaperone efficiency and an activity range greater than any other published so far (see section 4.4. Nanoparticle chaperones). These results will be interpreted in terms of the extent of the chaperone function that was found compared to that of αB-crystallin and the possible mechanism of this chaperone action. The second objective of this project was to improve the chaperone function of the nanoparticles with regions of αB-crystallin. This part was unsuccessful, and the reason for this will be investigated. These nanoparticles are not the first to be found to have chaperone activity; they will be put into the wider context of the field of nanoparticle chaperones and compared to those already in existence. Lastly, the potential implications of this work will be discussed, as well as suggestions for future work that could be done on this project.

4.1. Chaperone function of 'empty' nanoparticles

As predicted (see below), the nanoparticles used in this project showed the ability to function as a protein chaperone. The job of a protein chaperone is to prevent the aggregation of other proteins (section 1.2. Protein chaperones). Protein aggregation does not happen to properly folded proteins, it occurs when proteins are unfolded, misfolded or denatured (non-native), as this allows their hydrophobic regions to be exposed; they should be on the inside of the protein. However, when exposed, they bind to hydrophobic regions on other non-native proteins in an effort to avoid the solvent of the cell, and thus aggregation occurs. Protein chaperones prevent this aggregation by binding to the hydrophobic areas with their own hydrophobic domains, and so shielding them from binding to other non-native proteins. They either actively refold them with the aid of ATP (the chaperonins, HSP70, HSP90), or protect them until they can be refolded (the sHSPs); these are holdases.

The nanoparticles were predicted to function as protein chaperones because of their possible surface properties (see section 1.3.1. The Burkhard nanoparticles as chaperones). They were designed to efficiently self-assemble by the use of coiled-coils; each monomer consists of a pentameric coiled-coil region and trimeric coiled-coil region,

and when in the right conditions these oligomerise to form a 60-mer (Raman, Machaidze et al. 2006). These coiled-coils are stabilised by hydrophobic interactions (Burkhard, Stetefeld et al. 2001) and both contain other hydrophobic features: the pentameric coiled-coil contains a long hydrophobic indent (Malashkevich, Kammerer et al. 1996), whilst the trimeric coiled-coil has a hydrophobic seam (Burkhard, Meier et al. 2000) (Raman, Machaidze et al. 2006). Furthermore, their surface displayed proline-rich peptides (Figure 1.1D), which will lack secondary structure, as well as being neural; characteristics shared with the αB-crystallin C-terminal tails. Taken together, these features lead to our hypothesis that the nanoparticles could be able to act as protein chaperones.

This hypothesis was proved correct: the nanoparticles successfully chaperoned all three of the substrates used (section 3.3. Chaperone assays). However, they not only chaperoned the substrates, they chaperoned them to a remarkable extent, performing much better than the αB-crystallin control that was used. Their ability to chaperone aggregating proteins also stretched further than αB-crystallin in three directions. Firstly, they could still perform as a chaperone far beyond the minimum concentration of αB-crystallin needed for effective chaperoning. Reducing the concentration ratio of just 1:20 nanoparticle:citrate synthase only slightly affected the chaperone function, whereas doing the same to αB-crystallin removed all chaperone ability (Figure 3.3); this demonstrates a very efficient chaperone mechanism. It is probable that this efficiency is due to the symmetry of the nanoparticle. The surface hydrophobic regions that are likely to be responsible for the chaperone affect will be repeated 60 times on each particle, as the nanoparticles are made of 60 identical monomers. This would therefore create a very efficient chaperone.

Secondly, their chaperoning was not impaired by increased thermal stress. αB-crystallin could chaperone desmin aggregation at 37°C, but by 44°C the aggregation was too great, and no chaperoning was seen (Figure 3.7). The nanoparticles, however, chaperoned the filaments at 44°C to the same extent as 37°C, again, showing a high chaperoning efficiency. The temperature independence of the interactions between the nanoparticles and desmin was striking. At all three temperatures used (22°C, 37°C and 44°C) the low speed sedimentation assay indicated the nanoparticles were causing similar levels of filament-filament interactions, despite the differences seen for desmin alone.

This strange behaviour could be an insight into just how powerful these nanoparticles are; desmin aggregation caused by 44°C does not seem to present a problem for them, therefore they could perhaps chaperone a much higher level of aggregation. This could be tested by repeating these experiments at higher temperatures, or with a smaller concentration of nanoparticle relative to desmin.

Likewise, the high speed assay showed the same level of nanoparticle binding at all three temperatures, when more binding at a higher temperature would be expected. This could imply saturated binding at 22°C, which therefore would be very efficient substrate binding.

Thirdly, they have a much wider range of activity than αB-crystallin. They were effective from 22°C up to 70°C. This high temperature did not appear to effect the chaperoning of γ-crystallin; they still maintained almost complete chaperoning (Figure 3.4). This is a temperature at which most proteins would be denatured and lose activity, and so the fact that it has no effect on the activity of the nanoparticles is very impressive; it would be interesting to investigate just how big this range of activity is. αB-crystallin, however, has a much smaller activity range: 70°C would cause denaturing and loss of activity, and so clearly the nanoparticles out-perform αB-crystallin in this area.

4.2. Chaperone mechanism of 'empty' nanoparticles

As previously mentioned, there are four main mechanisms of chaperone action seen in mammal cells (section 1.2. Protein chaperones). The first is that of the chaperonins: the substrate binds to a hydrophobic active site within chamber, which subsequently undergoes a conformational change and causes the non-native protein to be refolded. Alternatively, HSP70 binds, with the aid of a co-chaperone, to a hydrophobic site on a nascent peptide and consequently causes the protein to fold. Similarly, HSP90 facilities a co-chaperone to bind to the peptide, but then uses a 'lid' closure to enable refolding. Lastly, the sHSPs simply play a protective role by binding to the substrate until it can be passed on to be refolded. The first three of these mechanisms utilise ATP to refold their

client protein, whereas the sHSPs differ, as they do not require ATP, but they are also not able to refold non-native peptides, and thus classed as holdases.

The nanoparticles used do not require ATP to function and show no evidence of being capable of refolding peptides (although this has not been tested); therefore it is likely that they are also holdases, and their mechanism of action most resembles that of the sHSPs. As already mentioned (section 1.3.1. The Burkhard nanoparticles as chaperones), they also show a structural similarity to the sHSPS: they are both spheres comprised of subunits, although the sHSP subunit is a dimer while the nanoparticle subunit is a trimer and/or a pentamer, as the monomers were designed with both trimeric and pentameric coiled-coils .

The mechanism of the sHSP chaperone function is not yet fully understood (section 1.2.4.2. The chaperone mechanism - αB-crystallin), although it is widely thought that substrate binding involves either subunit exchange, dissociation, conformational change or a mixture of the three, perhaps requiring activation (Haslbeck, Franzmann et al. 2005). It is known, however, that sHSP oligomers are dynamic, and thus constantly exchange subunits (Aquilina, Benesch et al. 2005), and SPR data has shown that increased subunit exchange leads to increased chaperoning (Liu, Ghosh et al. 2006). Conversely, however, a crosslinking study prevented subunit exchange did not prevent chaperone activity (Franzmann, Wuhr et al. 2005); therefore different sHSPs may use different chaperoning mechanisms.

It is unlikely that the nanoparticles use subunit exchange or dissociation for their mechanism of chaperone activity. This conclusion comes from their inability to be denatured by the process of boiling in SDS for running on a gel (section 3.2.1. Assembly of 'empty nanoparticle'). It suggests that the trimeric coiled-coils holding the subunits together are very strong, and so it seems unlikely that the subunits are dynamic. What seems more probable is that their chaperoning regions are constantly displayed on their surface and no activation is required to induce the chaperone activity. If activation was required for sHSP chaperoning and not for nanoparticle chaperoning, it could partly explain the nanoparticles' more efficient chaperoning ability.

4.3. Chaperone function of nanoparticles displaying αB-crystallin regions

A secondary hypothesis of this project was to investigate whether displaying regions of αB-crystallin known to be used in chaperoning improved their chaperone function. Unfortunately, however, testing this was impossible, as addition of these regions to the monomer resulted in precipitation and not nanoparticle formation. Four different αB-crystallin regions were used, but aggregation occurred in each case. The reason for this could be that the regions of αB-crystallin that bind to substrates are also oligomerisation domains. Consequently, all four of the regions used contained αB-crystallin oligomerisation domains (Figure 1.4), and so the αB-crystallin peptides bound to each other and thus prevented the formation of the nanoparticles. αB-crystallin forms oligomers of different sizes, usually about 24-mers. Here however, the monomers were expected to form 60-mers. The oligomerisation domains therefore will be packed much more densely than would be seen for αB-crystallin, and this could have been another factor that led to their aggregation.

To solve this problem, regions of αB-crystallin could be used which do not contain oligomerisation domains. These do tend to overlap with substrate binding domains, but from Figure 1.4 it can be seen that using amino acids 5-30 or 110-130 could solve this problem. Alternatively, a high-throughput screening (HTS) technique could be employed in which many sequences are tried and tested. Ones that did not lead to aggregation would then be tested for chaperone activity, and consequently the discovery of new substrate binding sites which are not involved in oligomerisation may give an insight into αB-crystallin's chaperone mechanism.

It is unlikely that if this was successful the nanoparticles would have improved chaperone function compared to the 'empty' nanoparticles because they appear to be a better chaperone than αB-crystallin itself. However, it would be useful by enabling more to be learnt about αB-crystallin, and perhaps in the future replace defective αB-crystallin in vivo.

4.4. Nanoparticle chaperones

This is not the first time that nanoparticles have been found to be good protein chaperones. They have several properties which lend themselves to this function, the most important being their relatively large surface area, which causes them to have good adsorption capabilities. Therefore they are able to bind to other molecules, which could be non-native proteins; thus being able to perform a holdase function (Fei and Perrett 2009). They also have the added advantage that their surfaces can usually be modified and so the surface properties can be optimised, potentially creating very efficient protein chaperones. Because of these factors several different nanoparticles have been designed with the purpose of creating an effective protein chaperone (section 1.2.5. Nanoparticle chaperones).

Some of these have metal cores. (De and Rotello 2008) De et al (De and Rotello 2008) created gold nanoparticles functionalised with dicarboxylate sidechains, which could chaperone three clients by using electrostatic interactions. In a similar mechanism, titanium oxide nanoparticles were effective on three substrates (Raghava, Singh et al. 2009). Magnetic ion nanoparticles have also been functionalised to have a chaperone function, although these have only been tested on one substrate (Badruddoza, Hidajat et al. 2010). All these nanoparticles not only prevented their clients from aggregating, but allow them to revert back to an active form. This is something that has not yet been tested with these nanoparticles; it would be exciting to see if they have the potential to restore enzymatic activity to their substrates.

Other chaperoning nanoparticles include micelles formed from amphiphillic polymers, which have a hydrophobic surface (Cavalieri, Chiessi et al. 2007), and a hydrogel of cholesteryl-group-bearing pullulan (CHP) (Nomura, Sasaki et al. 2005), both which have been found to have refolding ability on denatured carbonic anhydrase B (CAB), but with no results from further substrates yet.

The nanoparticles that have been made and tested in this project excel from the ones that have been published so far in their range of activity. The three chaperone assays put to them were all very different and highlighted different properties of their chaperoning. The tests done on the nanoparticles previously published so far have not

done this; even when different substrates were used, they were used under the same conditions, and highlighted their ability to aid the refolding of non-native proteins.

These peptide nanoparticles however are capable of more than that. In the citrate synthase assay (Figure 3.3) they showed that they are capable of complete chaperoning of a denatured substrate, at relatively normal conditions. This is comparable to the studies done on other nanoparticle chaperones. They were then tested at an extreme temperature in the γ-crystallin assay; where at 70ºC their ability to chaperone did not seem to be affected. This was a very impressive display of their robust nature. Lastly, they were successfully used in the desmin assay. This assay tested a completely different type of chaperoning: instead of preventing the aggregation of non-native proteins, they prevented filament-filament interactions from occurring. These filaments were not non-native proteins, and so clearly a different chaperone mechanism is required for this assay.

These nanoparticles are also the only protein nanoparticle chaperones. This makes them very easy to synthesise, and also makes them safer than the metal-based nanoparticles when considering potentially using them for applications in the body. They are therefore a very attractive alternative to the nanoparticle chaperones that have previously been published.

One more interesting feature of these nanoparticles is that they are the first that have been designed for an ulterior function yet have been discovered to have chaperone function. All of the others, therefore, have been designed with known principles of chaperoning in mind. This accidental property is thus very exciting; it could give a great new insight into the chaperone mechanism and so further investigation could lead to important findings.

4.5. Potential of this technology

Protein aggregation in the body is involved in many human diseases; known as protein aggregation diseases, examples of which include cataract, type 2 diabetes and neurodegenerative diseases such as Huntington's disease, Parkinson's disease and Alzheimer's disease. These diseases generally involve a complex, multistep process in

which protein aggregates become either ordered fibrils (amyloid) or amorphous deposites (Figure 4.1). These cannot be broken down, and are deposited; the composition and location of the deposits determines the disease (Bartolini and Andrisano 2010) (Dobson 2003). Consequently, there is great importance in the current research that is trying to find a way to prevent these aggregates from forming. Unfortunately, it is not simply a case of stopping proteins from aggregating; the proteins implicated in these diseases are usually defective in some way: either as the result of mutation or old age, and so simply chaperoning the protein does not solve the problem. However producing such effective protein chaperones as these gives a platform from which more research could proceed to perhaps in the future find a way to control production of these deposits. Furthermore, introducing chaperones in the early steps of these diseases could potentially slow down the progression of the diseases; in the case of aggregation diseases related to old age, this would greatly increase the quality of life for both the suffers and their carers. Using nanoparticle chaperones for this purpose instead of traditional drugs is convenient as their small size allows them to pass through the blood brain barrier (see section 1.1.1. Drug delivery), which is required when treating neurodegenerative diseases (Chopra, Gulati et al. 2008).

These nanoparticles have not yet been tested on amyloid fibrils however; there have been mixed results on the effects that nanoparticles can have on amyloid fibrils. Some nanoparticles have been found to retard the rate of fibrillogensis (Cabaleiro-Lago, Quinlan-Pluck et al. 2008) (Pai, Rubinstein et al. 2006), whereas other have been found actually increase it by accelerating the nucleation step, the rate limiting step (Wu, Sun et al. 2008) (Linse, Cabaleiro-Lago et al. 2007). This happens because the peptides are adsorbed to the nanoparticles' surface, making the peptide concentration very high and so promoting them to interact. However, it is also this adsorption that can reduce the fibrillogensis rate by blocking the active sites of the peptides. Therefore, further research needs to be carried out on these nanoparticles, as to whether they are effective on amyloid fibrils.

Whilst much is known about protein chaperones, there is still a great deal that is unknown. As mentioned previously, there are no synthetic nanoparticle chaperones that are similar to these; their peptide composition makes them unique. Therefore,

investigation into their exact method of aggregation inhibition could provide insights into the nature of the process by which protein aggregation occurs, particularly how amyloid fibrils form; knowledge which would indirectly aid the fight against protein aggregation diseases (Bartolini and Andrisano 2010).

The protein chaperone properties of these nanoparticles could also have a commercial application within the field of biotechnology. One example of how this would be used is as follows. As demonstrated in this project, bacteria are often used to overexpress recombinant proteins, yet up to 95% of the produced protein can form insoluble aggregates. This is usually dealt with by solubilising in a denaturant such as

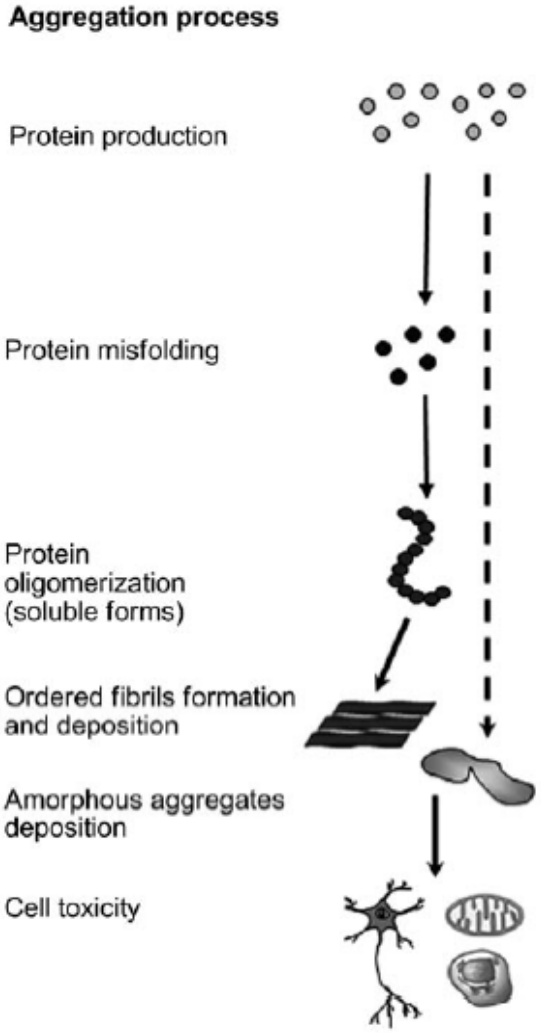

Figure 4.1 The protein aggregation process.
The steps involves in the development of protein into toxic deposits. Taken from (Bartolini and Andrisano 2010).

urea; alternatively aggregation could be prevented by using an artificial chaperone (Cavalieri, Chiessi et al. 2007). As they are robust, peptide-based, cheap and most importantly excellent chaperones, these nanoparticles would be perfect for such an application.

If this project were to continue, there is further work that could be done. More structural characterisation of the nanoparticles produced could be carried out to investigate their exact size and number of monomers. They could also undergo a heat denaturisation experiment, where they would be heated until they began to denature. This would give further information into how big their thermal range of activity is. Their exact chaperone mechanism could be determined and used in the production of chaperones in the future.

Research could also be done into their substrate range. It would be easy to test them on other general chaperone substrates such as insulin, CAB, papain and lysozyme. Their refolding potential on these substrates could also be investigated. They then could be tested on substrates that would require a different chaperone mechanism, such as pre-fibrillar proteins, as already mentioned.

The results from the desmin chaperone assay were very exciting as to the chaperone potential of these nanoparticles. More could be learnt from the assay, by lowering the relative nanoparticle concentration by increasing the temperature to push the nanoparticles further.

Lastly, as again already discussed, more work could be done on creating nanoparticles with αB-crystallin fragments displayed on their surface to investigate the effect that this could have and if it is possible to create an αB-crystallin 'super-chaperone'.

4.6. Conclusions

This project has uncovered a nanoparticle chaperone with great potential. It is very quick and easy to produce, adaptable by the modification of its monomers, and very robust. Most importantly however, it chaperones non-native proteins to a very high extent and has a wide activity range. Further research must now be carried out to determine the exact chaperone mechanism and thus to discover why the chaperoning is so remarkable. Work

must also be done to establish more substrates that these nanoparticles are effective on, especially pre-fibrillar proteins, in the hope that they can one day help to deal with protein aggregation diseases.

The project has made a very exciting discovery, and the implications of these results will be huge.

5. Bibliography

Agasti, S. S., S. Rana, M. H. Park, C. K. Kim, C. C. You and V. M. Rotello (2010). "Nanoparticles for detection and diagnosis." Advanced Drug Delivery Reviews **62**(3): 316-328.

Akiyoshi, K., Y. Sasaki and J. Sunamoto (1999). "Molecular chaperone-like activity of hydrogel nanoparticles of hydrophobized pullulan: Thermal stabilization with refolding of carbonic anhydrase B." Bioconjugate Chemistry **10**(3): 321-324.

Aquilina, J. A., J. L. P. Benesch, L. L. Ding, O. Yaron, J. Horwitz and C. V. Robinson (2005). "Subunit exchange of polydisperse proteins - Mass spectrometry reveals consequences of alpha A-crystallin truncation." Journal of Biological Chemistry **280**(15): 14485-14491.

Aquilina, J. A. and S. J. Watt (2007). "The N-terminal domain of alpha B-crystallin is protected from proteolysis by bound substrate." Biochemical and Biophysical Research Communications **353**(4): 1115-1120.

Augusteyn, R. C. (2004). "alpha-crystallin: a review of its structure and function." Clin Exp Optom **87**(6): 356-366.

Badruddoza, A. Z. M., K. Hidajat and M. S. Uddin (2010). "Synthesis and characterisation of β-cyclodextrin-conjugated magnetic nanoparticles and thier uses as solid-phase artificial chaperones in refolding of carbonic anhydrase bovine." Journal of Colloid and Interface Science **346**(2): 337-346.

Barratt, G. (2003). "Colloidal drug carriers: achievements and perspectives." Cellular and Molecular Life Sciences **60**(1): 21-37.

Bartolini, M. and V. Andrisano (2010). "Strategies for the Inhibition of Protein Aggregation in Human Diseases." Chembiochem **11**(8): 1018-1035.

Baschong, W., L. Hasler, M. Haner, J. Kistler and U. Aebi (2003). "Repetitive versus monomeric antigen presentation: direct visualization of antibody affinity and specificity." Journal of Structural Biology **143**(3): 258-262.

Boerman, O. C., W. J. G. Oyen, L. vanBloois, E. B. Koenders, J. W. M. vanderMeer, F. H. M. Corstens and G. Storm (1997). "Optimization of technetium-99m-labeled PEG liposomes to image focal infection: Effects of particle size and circulation time." Journal of Nuclear Medicine **38**(3): 489-493.

Bova, M. P., L. L. Ding, J. Horwitz and B. K. Fung (1997). "Subunit exchange of alphaA-crystallin." J Biol Chem **272**(47): 29511-29517.

Brinker, A., G. Pfeifer, M. J. Kerner, D. J. Naylor, F. U. Hartl and M. Hayer-Hartl (2001). "Dual function of protein confinement in chaperonin-assisted protein folding." Cell **107**(2): 223-233.

Burkhard, P., M. Meier and A. Lustig (2000). "Design of a minimal protein oligomerization domain by a structural approach." Protein Science **9**(12): 2294-2301.

Burkhard, P., J. Stetefeld and S. V. Strelkov (2001). "Coiled coils: a highly versatile protein folding motif." Trends in Cell Biology **11**(2): 82-88.

Cabaleiro-Lago, C., F. Quinlan-Pluck, I. Lynch, S. Lindman, A. M. Minogue, E. Thulin, D. M. Walsh, K. A. Dawson and S. Linse (2008). "Inhibition of Amyloid beta Protein Fibrillation by Polymeric Nanoparticles." Journal of the American Chemical Society **130**(46): 15437-15443.

Cavalieri, F., E. Chiessi and G. Paradossi (2007). "Chaperone-like activity of nanoparticles of hydrophobized poly(vinyl alcohol)." Soft Matter **3**(6): 718-724.

Chen, X., L. Lu, Z. Qi, H. Lu, J. Wang, X. X. Yu, Y. H. Chen and S. B. Jiang (2010). "Novel Recombinant Engineered gp41 N-terminal Heptad Repeat Trimers and Their Potential as Anti-HIV-1 Therapeutics or Microbicides." Journal of Biological Chemistry **285**(33): 25506-25515.

Chopra, D., M. Gulati, V. Saluja, P. Pathak and P. Bansal (2008). "Brain permeable nanoparticles." Recent Pat CNS Drug Discov **3**(3): 216-225.

Cohen-Sacks, H., Y. Najajreh, V. Tchaikovski, G. Gao, V. Elazer, R. Dahan, I. Gati, M. Kanaan, J. Waltenberger and G. Golomb (2002). "Novel PDGF beta R antisense encapsulated in polymeric nanospheres for the treatment of restenosis." Gene Therapy **9**(23): 1607-1616.

Crick, F. H. C. (1953). "The Packing of Alpha-Helices - Simple Coiled-Coils." Acta Crystallographica **6**(8-9): 689-697.

De, M. and V. M. Rotello (2008). "Synthetic "chaperones": nanoparticle-mediated refolding of thermally denatured proteins." Chemical Communications(30): 3504-3506.

Dobson, C. M. (2003). "Protein folding and misfolding." Nature **426**(6968): 884-890.

Ellis, R. J. (1994). "Molecular Chaperones - Opening and Closing the Anfinsen Cage." Current Biology **4**(7): 633-635.

Emerich, D. F. and C. G. Thanos (2006). "The pinpoint promise of nanoparticle-based drug delivery and molecular diagnosis." Biomolecular Engineering **23**(4): 171-184.

Fei, L. and S. Perrett (2009). "Effect of Nanoparticles on Protein Folding and Fibrillogenesis." International Journal of Molecular Sciences **10**(2): 646-655.

Ferrara, N. and H. P. Gerber (2001). "The role of vascular endothelial growth factor in angiogenesis." Acta Haematologica **106**(4): 148-156.

Feynman, R. (1960). "There's plenty of room at the bottom." Engineering and science: 22-36.

Franzmann, T. M., M. Wuhr, K. Richter, S. Walter and J. Buchner (2005). "The activation mechanism of Hsp26 does not require dissociation of the oligomer." J Mol Biol **350**(5): 1083-1093.

Ghosh, J. G. and J. I. Clark (2005). "Insights into the domains required for dimerization and assembly of human alpha B crystallin." Protein Science **14**(3): 684-695.

Ghosh, J. G., M. R. Estrada and J. I. Clark (2005). "Interactive domains for chaperone activity in the small heat shock protein, human alphaB crystallin." Biochemistry **44**(45): 14854-14869.

Ghosh, J. G., A. K. Shenoy, Jr. and J. I. Clark (2006). "N- and C-Terminal motifs in human alphaB crystallin play an important role in the recognition, selection, and solubilization of substrates." Biochemistry **45**(46): 13847-13854.

Gillies, E. R. and J. M. J. Frechet (2005). "Dendrimers and dendritic polymers in drug delivery." Drug Discovery Today **10**(1): 35-43.

Grislain, L., P. Couvreur, V. Lenaerts, M. Roland, D. Deprezdecampeneere and P. Speiser (1983). "Pharmacokinetics and Distribution of a Biodegradable Drug-Carrier." International Journal of Pharmaceutics **15**(3): 335-345.

Hartl, F. U. and M. Hayer-Hartl (2002). "Protein folding - Molecular chaperones in the cytosol: from nascent chain to folded protein." Science **295**(5561): 1852-1858.

Haslbeck, M. (2002). "sHsps and their role in the chaperone network." Cell Mol Life Sci **59**(10): 1649-1657.

Haslbeck, M., T. Franzmann, D. Weinfurtner and J. Buchner (2005). "Some like it hot: the structure and function of small heat-shock proteins." Nat Struct Mol Biol **12**(10): 842-846.

Haslbeck, M., A. Ignatiou, H. Saibil, S. Helmich, E. Frenzl, T. Stromer and J. Buchner (2004). "A domain in the N-terminal part of Hsp26 is essential for chaperone function and oligomerization." Journal of Molecular Biology **343**(2): 445-455.

Hayashi, T., S. Yamasaki, S. Nauenburg, T. Binz and H. Niemann (1995). "Disassembly of the reconstituted synaptic vesicle membrane-fusion complex in-vitro." Embo Journal **14**(10): 2317-2325.

Hayes, V. H., G. L. Devlin and R. A. Quinlan (2008). "Truncation of alphaB-crystallin by the myopathy-causing Q151X mutation significantly destabilizes the protein leading to aggregate formation in transfected cells." J Biol Chem.

Horwich, A. L., W. A. Fenton, E. Chapman and G. W. Farr (2007). "Two families of chaperonin: physiology and mechanism." Annu Rev Cell Dev Biol **23**: 115-145.

Horwitz, J. (2003). "Alpha-crystallin." Exp Eye Res **76**(2): 145-153.

Huang, C. C. and H. T. Chang (2007). "Parameters for selective colorimetric sensing of mercury(II) in aqueous solutions using mercaptopropionic acid-modified gold nanoparticles." Chemical Communications(12): 1215-1217.

Jakob, U., I. Meyer, H. Bugl, S. Andre, J. C. A. Bardwell and J. Buchner (1995). "Structural organization of prokaryotic and eukaryotic HSP90 - influence of divalent-cations on structure and fucntion." Journal of Biological Chemistry **270**(24): 14412-14419.

Jehle, S., P. Rajagopal, B. Bardiaux, S. Markovic, R. Kuhne, J. R. Stout, V. A. Higman, R. E. Klevit, B. Van Rossum and H. Oschkinat (2010). "Solid-state NMR and SAXS studies provide a structural basis for the activation of αB-crystallin oligomers." Nature Structural and Molecular Biology **17**(9): 1037-1042.

Kairemo, K., P. Erba, K. Bergstom and E. K. J. Pauwels (2008). "Nanoparticles in Cancer." Current Radiopharmaceuticals **1**: 30-36.

Kim, D. K. and J. Dobson (2009). "Nanomedicine for targeted drug delivery." Journal of Materials Chemistry **19**(35): 6294-6307.

Kim, K. K., R. Kim and S. H. Kim (1998). "Crystal structure of a small heat-shock protein." Nature **394**(6693): 595-599.

Laemmli, U. K. (1970). "Cleavage of Structural Proteins during Assembly of Head of Bacteriophage-T4." Nature **227**(5259): 680-&.

Lee, G. J. and E. Vierling (2000). "A small heat shock protein cooperates with heat shock protein 70 systems to reactivate a heat-denatured protein." Plant Physiol **122**(1): 189-198.

Leesmiller, S. P. and C. W. Anderson (1989). "The human doublt-standard DNA-activated proetin-kinase phosphorylates the 90-kDa heat-shock protein, HSP90-alpha at 2 NH2-terminal threonine residues." Journal of Biological Chemistry **264**(29): 17275-17280.

Lindner, R. A., A. Kapur, M. Mariani, S. J. Titmuss and J. A. Carver (1998). "Structural alterations of alpha-crystallin during its chaperone action." Eur J Biochem **258**(1): 170-183.

Linse, S., C. Cabaleiro-Lago, W. F. Xue, I. Lynch, S. Lindman, E. Thulin, S. E. Radford and K. A. Dawson (2007). "Nucleation of protein fibrillation by nanoparticles."

Proceedings of the National Academy of Sciences of the United States of America **104**(21): 8691-8696.

Liu, J., A. L. Levine, J. S. Mattoon, M. Yamaguchi, R. J. Lee, X. L. Pan and T. J. Rosol (2006). "Nanoparticles as image enhancing agents for ultrasonography." Physics in Medicine and Biology **51**(9): 2179-2189.

Liu, L., M. A. Zern, M. E. Lizarzaburu, M. H. Nantz and J. Wu (2003). "Poly(cationic lipid)-mediated in vivo gene delivery to mouse liver." Gene Therapy **10**(2): 180-187.

Liu, L. Y., J. G. Ghosh, J. I. Clark and S. Y. Jiang (2006). "Studies of alpha B crystallin subunit dynamics by surface plasmon resonance." Analytical Biochemistry **350**(2): 186-195.

Lucent, D., J. England and V. Pande (2009). "Inside the chaperonin toolbox: theoretical and computational models for chaperonin mechanism." Physical Biology **6**(1): -.

Lutsiak, M. E. C., D. R. Robinson, C. Coester, G. S. Kwon and J. Samuel (2002). "Analysis of poly(D,L-lactic-co-glycolic acid) nanosphere uptake by human dendritic cells and macrophages in vitro." Pharmaceutical Research **19**(10): 1480-1487.

Malashkevich, V. N., R. A. Kammerer, V. P. Efimov, T. Schulthess and J. Engel (1996). "The crystal structure of a five-stranded coiled coil in COMP: A prototype ion channel?" Science **274**(5288): 761-765.

Mchaourab, H. S., J. A. Godar and P. L. Stewart (2009). "Structure and Mechanism of Protein Stability Sensors: Chaperone Activity of Small Heat Shock Proteins." Biochemistry **48**(18): 3828-3837.

McLaughlin, S. H., H. W. Smith and S. E. Jackson (2002). "Stimulation of the weak ATPase activity of human Hsp90 by a client protein." Journal of Molecular Biology **315**(4): 787-798.

Medintz, I. L., H. T. Uyeda, E. R. Goldman and H. Mattoussi (2005). "Quantum dot bioconjugates for imaging, labelling and sensing." Nature Materials **4**(6): 435-446.

Meimaridou, E., S. B. Gooljar and J. P. Chapple (2009). "From hatching to dispatching: the multiple cellular roles of the Hsp70 molecular chaperone machinery." Journal of Molecular Endocrinology **42**(1-2): 1-9.

Moghimi, S. M., A. C. Hunter and J. C. Murray (2001). "Long-circulating and target-specific nanoparticles: Theory to practice." Pharmacological Reviews **53**(2): 283-318.

Nakamoto, H. and L. Vigh (2007). "The small heat shock proteins and their clients." Cellular and Molecular Life Sciences **64**(3): 294-306.

Nomura, Y., M. Ikeda, N. Yamaguchi, Y. Aoyama and K. Akiyoshi (2003). "Protein refolding assisted by self-assembled nanogels as novel artificial molecular chaperone." Febs Letters **553**(3): 271-276.

Nomura, Y., Y. Sasaki, M. Takagi, T. Narita, Y. Aoyama and K. Akiyoshi (2005). "Thermoresponsive controlled association of protein with a dynamic nanogel of hydrophobized polysaccharide and cyclodextrin: Heat shock protein-like activity of artificial molecular chaperone." Biomacromolecules **6**(1): 447-452.

Otsuka, H., Y. Akiyama, Y. Nagasaki and K. Kataoka (2001). "Quantitative and reversible lectin-induced association of gold nanoparticles modified with alpha-lactosyl-omega-mercapto-poly(ethylene glycol)." Journal of the American Chemical Society **123**(34): 8226-8230.

Pai, A. S., I. Rubinstein and H. Onyuksel (2006). "PEGylated phospholipid nanomicelles interact with beta-amyloid((1-42)) and mitigate its beta-sheet formation, aggregation and neurotoxicity in vitro." Peptides **27**(11): 2858-2866.

Papapostolou, D. and S. Howorka (2009). "Engineering and exploiting protein assemblies in synthetic biology." Mol Biosyst **5**(7): 723-732.

Peek, L. J., C. R. Middaugh and C. Berkland (2008). "Nanotechnology in vaccine delivery." Advanced Drug Delivery Reviews **60**(8): 915-928.

Perez, C., A. Sanchez, D. Putnam, D. Ting, R. Langer and M. J. Alonso (2001). "Poly(lactic acid)-poly(ethylene glycol) nanoparticles as new carriers for the delivery of plasmid DNA." Journal of Controlled Release **75**(1-2): 211-224.

Pimentel, T. A. P. F., Z. Yan, S. A. Jeffers, K. V. Holmes, R. S. Hodges and P. Burkhard (2009). "Peptide Nanoparticles as Novel Immunogens: Design and Analysis of a Prototypic Severe Acute Respiratory Syndrome Vaccine." Chemical Biology & Drug Design **73**(1): 53-61.

Raghava, S., P. K. Singh, A. R. Rao, V. Dutta and M. N. Gupta (2009). "Nanoparticles of unmodified titanium dioxide facilitate protein refolding." Journal of Materials Chemistry **19**(18): 2830-2834.

Rajagopal, K. and J. P. Schneider (2004). "Self-assembling peptides and proteins for nanotechnological applications." Curr Opin Struct Biol **14**(4): 480-486.

Raman, S., G. Machaidze, A. Lustig, U. Aebi and P. Burkhard (2006). "Structure-based design of peptides that self-assemble into regular polyhedral nanoparticles." Nanomedicine **2**(2): 95-102.

Roco, M. C. (2003). "Nanotechnology: convergence with modern biology and medicine." Current Opinion in Biotechnology **14**(3): 337-346.

Saibil, H. R. (2008). "Chaperone machines in action." Current Opinion in Structural Biology **18**(1): 35-42.

Scheufler, C., A. Brinker, G. Bourenkov, S. Pegoraro, L. Moroder, H. Bartunik, F. U. Hartl and I. Moarefi (2000). "Structure of TPR domain-peptide complexes: Critical elements in the assembly of the Hsp70-Hsp90 multichaperone machine." Cell **101**(2): 199-210.

Schroeder, U., A. Graff, S. Buchmeier, P. Rigler, U. Silvan, D. Tropel, B. M. Jockusch, U. Aebi, P. Burkhard and C. A. Schoenenberger (2009). "Peptide Nanoparticles Serve as a Powerful Platform for the Immunogenic Display of Poorly Antigenic Actin Determinants." Journal of Molecular Biology **386**(5): 1368-1381.

Singh, R. and J. W. Lillard (2009). "Nanoparticle-based targeted drug delivery." Experimental and Molecular Pathology **86**(3): 215-223.

Spiess, C., A. S. Meyer, S. Reissmann and J. Frydman (2004). "Mechanism of the eukaryotic chaperonin: protein folding in the chamber of secrets." Trends in Cell Biology **14**(11): 598-604.

Sun, Y. and T. H. MacRae (2005). "Small heat shock proteins: molecular structure and chaperone function." Cell Mol Life Sci **62**(21): 2460-2476.

Thaxton, C. S., D. G. Georganopoulou and C. A. Mirkin (2006). "Gold nanoparticle probes for the detection of nucleic acid targets." Clinica Chimica Acta **363**(1-2): 120-126.

Thomas, T. P., I. J. Majoros, A. Kotlyar, J. F. Kukowska-Latallo, A. Bielinska, A. Myc and J. R. Baker (2005). "Targeting and inhibition of cell growth by an engineered dendritic nanodevice." Journal of Medicinal Chemistry **48**(11): 3729-3735.

van Montfort, R. L., E. Basha, K. L. Friedrich, C. Slingsby and E. Vierling (2001). "Crystal structure and assembly of a eukaryotic small heat shock protein." Nat Struct Biol **8**(12): 1025-1030.

Wandinger, S. K., K. Richter and J. Buchner (2008). "The Hsp90 chaperone machinery." Journal of Biological Chemistry **283**(27): 18473-18477.

Weissman, J. S., Y. Kashi, W. A. Fenton and A. L. Horwich (1994). "groel-mediated protein-folding proceeds by multiple rounds of binding and release of nonnative forms." Cell **78**(4): 693-702.

Witt, S. N. (2010). "Hsp70 Molecular Chaperones and Parkinson's Disease." Biopolymers **93**(3): 218-228.

Wu, W. H., X. Sun, Y. P. Yu, J. Hu, L. Zhao, Q. Liu, Y. F. Zhao and Y. M. Li (2008). "TiO2 nanoparticles promote beta-amyloid fibrillation in vitro." Biochemical and Biophysical Research Communications **373**(2): 315-318.

Young, J. C., J. M. Barral and F. U. Hartl (2003). "More than folding: localized functions of cytosolic chaperones." Trends in Biochemical Sciences **28**(10): 541-547.

Zhang, Y., F. Schlachetzki and W. M. Pardridge (2003). "Global non-viral gene transfer to the primate brain following intravenous administration." Molecular Therapy **7**(1): 11-18.

Zolnik, B. S. and N. Sadrieh (2009). "Regulatory perspective on the importance of ADME assessment of nanoscale material containing drugs." Advanced Drug Delivery Reviews **61**(6): 422-427.